



**RESEARCH ARTICLE**

10.1029/2018EA000378

**Special Section:**

Science and Exploration of the Moon, Near-Earth Asteroids, and the Moons of Mars

This article is a companion to Ito et al. (2018), <https://doi.org/10.1029/2018EA000375>.

**Key Points:**

- Advancements in field portable technologies have the capability to increase the science return from crewed planetary surface missions
- Simulated extravehicular activities were conducted in planetary analog sites to investigate the utility of portable instruments
- More integrated testing is needed to evaluate varying modes of integrating field portable instruments beyond a handheld capacity

**Correspondence to:**

K. E. Young,  
kelsey.e.young@nasa.gov

**Citation:**

Young, K. E., Bleacher, J. E., Rogers, A. D., Schmitt, H. H., McAdam, A. C., Garry, W. B., et al. (2018). The incorporation of field portable instrumentation into human planetary surface exploration. *Earth and Space Science*, 5, 697–720. <https://doi.org/10.1029/2018EA000378>

Received 15 FEB 2018

Accepted 24 AUG 2018

Accepted article online 12 SEP 2018

Published online 5 NOV 2018

©2018. The Authors.

This is an open access article under the terms of the Creative Commons

Attribution-NonCommercial-NoDerivs License, which permits use and distribution in any medium, provided the original work is properly cited, the use is non-commercial and no modifications or adaptations are made.

This article has been contributed to by U.S. Government employees and their work is in the public domain in the USA.

# The Incorporation of Field Portable Instrumentation Into Human Planetary Surface Exploration

K. E. Young<sup>1</sup> , J. E. Bleacher<sup>1</sup>, A. D. Rogers<sup>2</sup> , H. H. Schmitt<sup>3</sup>, A. C. McAdam<sup>1</sup>, W. B. Garry<sup>1</sup>, P. L. Whelley<sup>4</sup>, S. P. Scheidt<sup>5</sup>, G. Ito<sup>2</sup> , C. A. Knudson<sup>4</sup> , T. G. Graff<sup>6</sup>, L. V. Bleacher<sup>1</sup>, N. Whelley<sup>4</sup>, C. A. Evans<sup>7</sup>, J. M. Hurtado Jr.<sup>8</sup>, and T. D. Glotch<sup>2</sup> 

<sup>1</sup>NASA Goddard Space Flight Center, Greenbelt, MD, USA, <sup>2</sup>Department of Geosciences, Stony Brook University, Stony Brook, NY, USA, <sup>3</sup>Department of Engineering Physics, University of Wisconsin-Madison, Albuquerque, NM, USA, <sup>4</sup>College Park/CRESST Cooperative Agreement at NASA Goddard Space Flight Center, University of Maryland, Greenbelt, MD, USA, <sup>5</sup>University of Arizona, Tucson, AZ, USA, <sup>6</sup>Jacobs JETS Contract, NASA Johnson Space Center, Houston, TX, USA, <sup>7</sup>NASA Johnson Space Center, Houston, TX, USA, <sup>8</sup>University of Texas at El Paso, El Paso, TX, USA

**Abstract** Field portable instrumentation, such as in situ geochemical analyzers or broader field of view instruments like multispectral imagers or other imaging capabilities, has the potential to dramatically increase the science return of a planetary surface exploration mission. However, more work is needed to determine how emerging portable technologies should be designed and implemented into evolving mission architectures. This work summarizes the efforts of the RIS<sup>4</sup>E (Remote, In Situ and Synchrotron Studies for Science and Exploration) SSERVI (Solar System Exploration Research Virtual Institute) team in investigating how field portable instruments should be including into planning for future exploration EVAs (extravehicular activities). EVA crews of geologists and astronauts tested a variety of portable and handheld technologies at both the December 1974 lava flow, Kilauea Volcano, Hawai'i, and Kilbourne Hole, New Mexico, both of which are planetary analog sites. The timeline data gathered during instrument deployment were then mapped onto EVA timelines used in large-scale NASA planetary surface exploration analog missions. Results and recommendations for future instrument hardware and software development are discussed, as is the operational framework necessary for incorporating in situ analytical capabilities into future planetary surface exploration.

## 1. Introduction

The six Apollo lunar surface missions from 1969 to 1972 included 12 astronauts conducting a series of extravehicular activities (EVAs) designed to explore six different lunar landing sites. These EVAs were relatively short (ranging between approximately 2.5–7.5 hr), tightly scheduled, and the astronauts were able to collect a wide variety of samples and scientific data for return to Earth (Miller et al., 2016). However, the technology deployed by the Apollo astronauts was limited to tools designed only for sample collection and storage (i.e., tongs, scoops, hammers, and sample bags; Allton, 1989). Experiment packages like the EASEP (Early Apollo Scientific Experiments Package) and the ALSEP (Apollo Lunar Surface Experiments Packages) were also deployed during the Apollo missions, but these were designed for long-term monitoring of the lunar surface after the departure of the crew, and none of the data were accessible to the astronauts during their missions. Finally, the later three Apollo missions (15, 16, and 17) included the use of the Lunar Roving Vehicle (LRV), a rover designed to carry the astronauts, their tools, and all samples collected during EVA. The LRV enabled the crews to travel much longer distances (approximately 20 km on the longest EVA, conducted during Apollo 17) and also reduced the load each astronaut was responsible for carrying, making it a valuable tool for exploration (Williams, 2005).

In the over 40 years since Apollo 17 departed from the lunar surface, significant advancements have been made in field portable technologies. These innovations have opened up new capabilities for field explorers, both on Earth and on other planetary surfaces. In traditional terrestrial field geologic campaigns, geologists visit a site of interest in order to explore, map, and collect samples (Frodeman, 1995; Hodges & Schmitt, 2011; Kastens et al., 2009). These samples are then returned for follow-up laboratory analysis, which often takes weeks to months to conduct. The resulting data are assimilated and it is frequently the case that subsequent field campaigns are conducted in order to more fully address all relevant science questions posed about the

site. Subsequent field campaigns may even be designed to address new questions about the site that would not have been posed but for detailed laboratory analyses of the returned samples. On extraterrestrial surfaces, return trips are not normally feasible and thus it is crucial to maximize the efficiency of the time spent during a planetary surface mission. Similar constraints can exist for remote sites on Earth. Recent advancements in field portable instrumentation can provide crews with increased real-time data, maximizing the scientific productive of time onsite. Ultimately, it is critical that instruments rapidly provide an explorer with more knowledge and enable decision making in near-real time. However, the tradeoffs between instrument weight, ease of use, and the incorporation of data into field operations are not yet clearly characterized for the type of instrumentation currently in development for field science. Thus, understanding how these tools should be designed and how they could fit into planetary surface operations is still limited, and this knowledge gap must be addressed before decisions are made on what technologies should be included on future missions and whether they will be more useful in the field or in more leisurely examination in a habitat.

This work provides an overview of how new developments in field-deployable instruments can fit in to a planetary surface exploration architecture, and, most importantly, what effects these technologies have on EVA timelines and potential scientific returns. The RIS<sup>4</sup>E (Remote, In Situ and Synchrotron Studies for Science and Exploration) SSERVI (Solar System Exploration Research Virtual Institute) team has conducted a series of field campaigns in two relevant analog environments, the December 1974 (D1974) flow at Kilauea Volcano on the Big Island, Hawaii, and the Kilbourne Hole structure in the Potrillo Volcanic Field, New Mexico. The primary goal of these campaigns was to investigate how field portable instruments impact crewed planetary surface exploration timelines and relevant mission architectures and thereby test the competing hypotheses that portable instruments do or do not enhance the science return of an EVA-based human exploration mission. Lessons learned can be used to better develop new instruments and to evolve exploration architectures.

We discuss a variety of instruments field tested in both planetary analog environments, their deployment procedures, the time required to operate each instrument and assimilate the data, and how the instruments might work together to enhance the efficiency and productivity of planetary explorers. It should be noted that the instruments chosen for this study are certainly not the only options for inclusion in future surface missions. Their selection was driven by the need for a comprehensive look at the geology of a site, including chemistry, mineralogy, spectral characteristics, surface texture, subsurface structures, and surface morphology. Many of the measurements described here have been made both in terrestrial field applications as well as on Mars rover missions using instruments operating with comparable technologies. Detailed scientific results from these deployments are presented in other publications (e.g., Yant et al., 2018) and deal with the geologic history and evolution of these analog terrains.

A critical question to be answered, before field portable instruments are assigned to an exploration activity, is, "Will their use increase or reduce the scientific return versus the time lost in knowledgeable examination of the context of collected samples that can be studied with similar instruments within a habitat"?

## 2. Overall Mission Architecture

As we investigate each technology and how it can fit into a crewed planetary exploration mission, we do so based on assumptions of human exploration architectures that are under continued investigation by NASA analog field technology tests. By integrating our instruments in an architecture concept supported by numerous other field tests, we develop a robust understanding of the effect that instrument incorporation has on the overall mission timeline by extrapolating from the larger analog mission timelines, without having the overhead of complex and expensive integrated field tests that are scheduled infrequently. Therefore, we focus specifically on EVA timeline duration as affected by the isolated variable of portable instrument operation. Two of the fully integrated tests (including habitat and rover deployment, simulated EVAs with science objectives comparable to those expected in planetary exploration, and an immersive analog environment that has a crew living full time in the habitat or rover) that have been used for planning for future surface exploration are the NASA Desert RATS (Research and Technology Studies) and NEEMO (NASA Extreme Environments Mission Operations) testing programs.

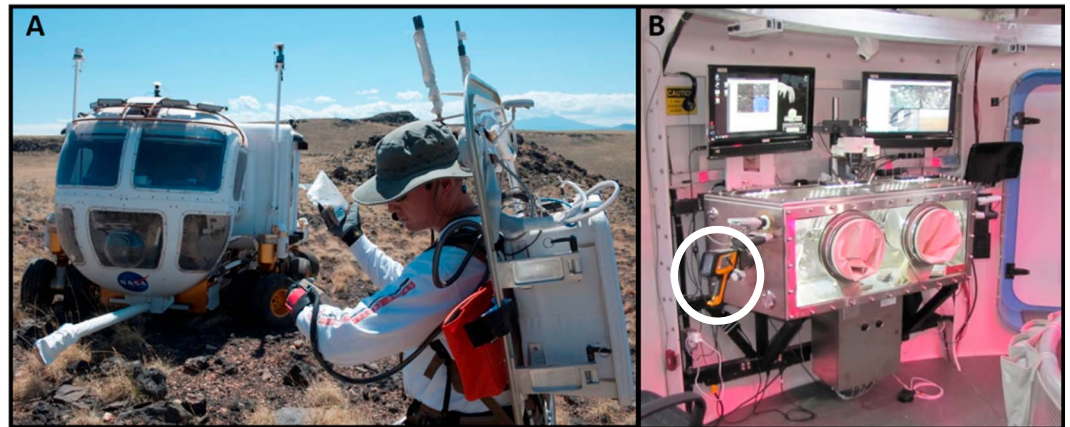


**Figure 1.** Planetary surface exploration concepts were tested extensively during multiple Desert RATS missions. While instruments were not operated during EVA, crews were able to collect high-resolution data inside of GeoLab, their habitat laboratory. (a) Desert RATS 2011 crewmember, NASA Astronaut Kjell Lindgren, works with a collected sample during EVA. In the Desert RATS mission architecture, crews could bring collected samples into the GeoLab facility for detailed analysis while on a planetary surface. (b) The GeoLab facility is shown. Working inside the glovebox, crews examined collected samples with a microscope and analytical technologies. Shown mounted on the left side of GeoLab is the hXRF spectrometer (circled in white), capable of collecting real-time geochemical data for analysis by the crew and science support teams on “Earth.”

### 2.1. The NASA Desert RATS Field Trials

The NASA Desert RATS field tests were conducted yearly between 1997 and 2012 in planetary analog sites such as the San Francisco Volcanic Field (SFVF) in Arizona and the Space Vehicle Mockup Facility at NASA’s Johnson Space Center (JSC; Eppler et al., 2013; Ross et al., 2013). Many technologies and operational scenarios were tested using the Multi Mission Space Exploration Vehicle (MMSEV) to explore areas within the SFVF (Abercromby et al., 2013). The MMSEV is a pressurized rover designed to support a human crew for days and weeks at a time on traverses at other planetary destinations, whether it be the Moon, Mars, or an asteroid (Figure 1a). For example, in one operational architecture tested during the 2-week 2010 field test, two rovers explored the SFVF together, each with two crewmembers (one astronaut or engineer and one field geologist). Young et al. (2013) describes the tools and technologies used in the 2010 field trial, which included sample collection tools similar to those deployed during Apollo. Hurtado et al. (2013) and Bleacher et al. (2013) discuss the manner in which this MMSEV-based exploration strategy can be used to maximize science return and Young et al. (2013) introduces recommendations for instrument development that could further enhance achievable science in the same mission style. These recommendations highlight the need for testing the use of higher spatial resolution instrumentation in preparation for possible use during the next generation of planetary exploration, a niche addressed in this study.

Evans et al. (2013) discuss an alternate use for some of these in situ technologies through integration in GeoLab, a habitat laboratory designed for extended stays at another planetary body. For example, GeoLab in the 2010 Desert RATS test contained a glovebox for examining geologic samples of interest during an extended planetary surface stay (Figure 1b). The architecture under consideration was a crew in a Constellation-style mission, staying on the surface for weeks or even months at a time. These long stays would allow for multiday traverses away from the habitat in the MMSEV. When the crew was in the habitat, however, they could spend their time partially on initial analyses of samples collected during prior traverses in an effort to both high grade samples for return to Earth and to learn more about the exploration zone’s geology, enabling evolution of future traverses. The glovebox contained cameras for sending back images of the samples to science support teams on Earth, as well as a handheld X-ray fluorescence spectrometer (hXRF) to allow for real-time geochemical data acquisition, which could also be transmitted to “Earth” (or in this case, to science support teams back in Mission Control). Although Desert RATS was not able to test field incorporation of portable instruments into a planetary EVA, they did test the incorporation of these technologies into a planetary mission scenario. The next step identified from these studies was to deploy a suite of instruments in the field during geologic campaigns and simulated

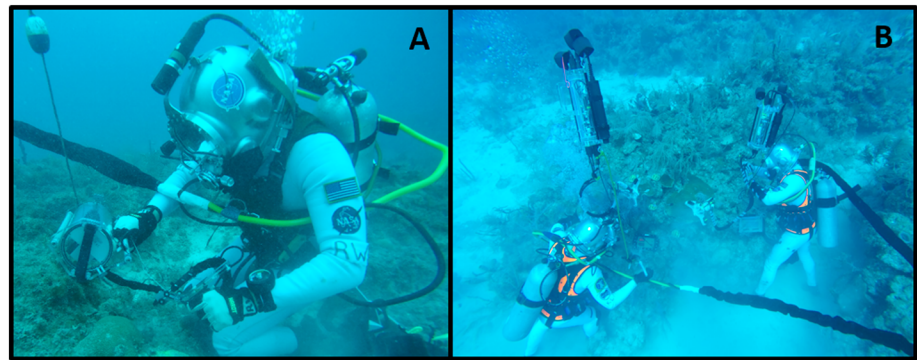


**Figure 2.** Recent NEEMO missions have explored the use of field portable instrumentation during EVA following input on operational strategies from smaller field tests (e.g., RIS<sup>4</sup>E). (a) A NEEMO 21 crewmember deploys the PAM fluorometer, an instrument operating on the same time scales and in a similar handheld mode as the hXRF instrument. (b) Two NEEMO 22 crewmembers deploy two CISME instruments (Coral In Situ Metabolism) during an EVA. This instrument takes much longer to set up and integrate, comparable to the portable XRD instrument. NEEMO 22 explored having a two-person crew use both one and two of these portable instruments at a site of interest, which resemble XRD instruments from the perspective of time resources.

EVA and evaluate the cost added to a mission timeline against the science value added to that mission (Young et al., 2013).

## 2.2. NEEMO

The NASA NEEMO team has completed 22 successful missions in the Aquarius habitat, the only underwater research station in the world. Located 6 miles offshore from Islamorada, Florida, in approximately 60 feet of water, the Aquarius habitat is a unique analog for spaceflight. Crews live in isolation in an extreme environment and are able to test both intravehicular (IV) and extravehicular (EV) tasks, simulating mission architectures that include orbiting space stations (i.e., the International Space Station), surface habitat laboratories, and surface missions with EVA capabilities. Crews conduct multi-hour EVAs with high fidelity science objectives. Though primary NEEMO science objectives are focused on marine science (e.g., Bonthond et al., 2018), the sample collection and curation procedures are designed to closely resemble current operational concepts for future planetary surface exploration and provide a development platform for testing new protocols and EVA technologies (e.g., portable instrument deployment, EVA informatics, IV support system capabilities, communications structures, etc., Graff et al., 2017; Young et al., 2018). Recent NEEMO objectives have also focused on advanced curation concepts for future spaceflight. Additionally, NEEMO has tested in situ analytical technologies in recent missions that are comparable in deployment procedures to several of the instruments deployed in this study. Specifically, two instruments deployed during NEEMO 21 (2016) and 22 (2017) have direct relevance to hXRF and X-ray diffraction (XRD) instruments in their operational modes and strategies (Figure 2). The general operational concept for NEEMO EVA Science is comparable to the EVA methodology used in Desert RATS. Crews egress from the habitat (rather than the MMSEV) and conduct science tasks during their EVA, including site reconnaissance and general exploration, sampling, and instrument operations. They are aided by an IV crewmember inside the habitat, as well as science support teams on 'Earth' (in the shore-based facility) who can advise them on sampling priorities and other science objectives. NEEMO builds off of Desert RATS missions in that the crew operates instruments during EVAs (Figure 2), and instrument procedures and troubleshooting tips are viewable on an EVA informatics system, called Cue Cards, which also contain sampling procedures, tips on identifying high priority samples, and procedures for using all technology available for EVA. RIS<sup>4</sup>E SSERVI work is unique in that it both leverages past integrated operational field tests (like Desert RATS and NEEMO) but also feeds operational lessons and recommendations into ongoing tests and operational missions like NEEMO. This relationship between analog field tests and future surface exploration will be discussed in detail later in this manuscript.

## 2.3. The Mission Simulation Scenario

During the Desert RATS 2010 test, the rover crews followed a specific procedure when conducting EVAs. For this study, we adopt a similar methodology, as the strategy developed during Desert RATS EVAs, which is

likely to be comparable to operational strategies for EVAs conducted on other planetary surfaces. This Desert RATS and RIS<sup>4</sup>E methodology was as follows: Once an EVA site was selected through a combination of pre-mission planning using remotely sensed data, crew insight from any EVAs conducted earlier in the mission, and from ongoing conversations between the crew and any science support teams, the two-person crew would drive the rover (or, in the case of RIS<sup>4</sup>E, the crew would walk up to the site along a path the crew deemed appropriate for the physical limitations of the MMSEV) up in front of the outcrop or target of interest. After parking the rover, the crew discussed the science and sampling plan for the EVA and divided up EVA tasks among each other. They also initiated a series of images of the site taken with cameras mounted on the rover (or for RIS<sup>4</sup>E EVAs, initiated comparable analyses by communicating with the relevant instrument teams, as discussed below). In this way they generated a data product on top of which they could take notes about their EVA and display in situ instrument data once they completed all EVA activities (e.g., site exploration and sampling) and returned back to and entered the rover. For example, panoramic images taken with a Gigapan system (a high-resolution panoramic imaging system; Young et al., 2013) in the Desert RATS tests could be annotated with sampling locations once the crew returned to the rover. The crew acquired these panoramic images while they were preparing to exit the rover to ensure that they would not obscure the field of view while conducting operations. After these preparatory steps were complete, the crew egressed. Once they were out of the rover, the crew collected all hardware from the rover necessary for the planned EVA tasks (sampling technologies, curation tools, etc.) and started the EVA.

By using full mission simulations as the reference design architecture for this study, and focusing only on EVA activities (e.g., not including rover operations), we ensure that the introduction of instrument operations remains a new and isolated variable to complement the larger Desert RATS and NEEMO tests (the former of which did not include field deployment of instruments and the latter of which combined a variety of other EVA objectives with portable instrument deployment, making it challenging to isolate that as a test variable). Both RIS<sup>4</sup>E deployments utilized a mission architecture that included large field of view instruments that collect data on an outcrop scale and smaller, higher-resolution instruments that target in situ chemistry and mineralogy, operated in a hands-on mode by the EV crew. EV crews simulated the use of approaching an EVA site in a rover by simply walking up to a site deemed to be appropriate for where they would park a rover in a Desert RATS-style mission, the criteria for which included a spot large enough to park the MMSEV that was level and free of large obstructions (boulders, cracks, etc.).

The RIS<sup>4</sup>E team completed two field deployments at lunar and martian analog environments where simulated EVAs with instrumentation were conducted. In both cases these EVAs took place over multiple days. The first two EVAs were conducted during 1 day at each field site, and these EVAs were followed by a “data processing day,” where the crew had time to review all the data they collected the day before, to interact with a science team, and plan for subsequent EVAs. While they also had access to some of the data during the EVA where they collected it, the follow-up day for focused data processing and examination simulated how the crew in a planetary surface exploration mission would have time overnight, either in a lander, rover, or habitat laboratory, to review the data and discuss it in preparation for future work. Or, if time to review data was not offered to the crew, this time would enable a crew to receive feedback from science support teams on Earth, who would surely be working to process each EVA’s data overnight after it was collected. Though RIS<sup>4</sup>E deployments did not include real-time science support analogous to a science backroom (like those present during each Apollo surface mission and during NEEMO missions), the data processing day enabled us to retain this crucial data assimilation time, as well as to iterate on data visualization products (see Section 4.2).

### **2.3.1. The SSERVI RIS<sup>4</sup>E Field Sites**

RIS<sup>4</sup>E field sites were chosen due to the host of intriguing science questions at each location as well as to their analog properties relating them to comparable surface processes on the lunar and martian surfaces. All RIS<sup>4</sup>E EVAs were designed not only to deploy field portable instrumentation but also to investigate the geologic history of this analog field sites.

#### **2.3.1.1. The December 1974 (D1974) Lava Flow, Kilauea Volcano, HI**

Erupted over a course of approximately 6.5 hours in the SW rift zone of Kilauea Volcano (Lockwood et al., 1999; Soule et al., 2004), the D1974 lava flow has been identified and used as a planetary analog flow by several groups. The low slope morphology of the D1974 flow and the SW rift zone in general is analogous to volcanic terrains on both the lunar and martian surface and has been used to as an analog to understand physical lava flow emplacement on Mars (Bleacher et al., 2015; Hamilton et al., 2015) due to the variety of

flow textures and structures that are preserved (Soule et al., 2004) and remain unburied within this short-lived flow event. Additionally, this environment includes long-lived sites of fumarolic activity (Sutton & Elias, 2014) that has contributed to host rock alteration in the region, which has served as a basis for interpreting martian data (Chemtob et al., 2010; Seelos et al., 2010). The local environment of the D1974 flow is an arid climate in the Ka'ū Desert that experiences occasional damp periods. The interaction of limited precipitation with the D1974 flow, along with the proximity of the flow to the active caldera, with the basaltic composition produces alteration materials (Schiffman et al., 2006), which are comparable to those identified recently by the martian rovers (Chemtob et al., 2010; Seelos et al., 2010). Additionally, like the majority of the martian surface, almost all of the materials at the site are volcanic in origin. This includes the basaltic lava flows (both the D1974 flow and the older flow underneath it), volcanoclastic sediments eroded by fluvial and eolian processes and deposited in and around the flow, and tephra, both lapilli and fine basaltic glass strands (e.g., Pele's hair).

Three EVAs were conducted at the D1974 flow in May/June of 2015 to characterize each EVA site and collect a suite of samples representing the geologic, geochemical, and mineralogical variability at each site. Major science objectives for each of the three EVAs at the D1974 flow were to: characterize the composition of the flow, evaluate the morphology and emplacement history of the flow, and to determine the alteration history of the flow postemplacement. Instruments used during this deployment were LiDAR (light detection and ranging), an infrared spectral imager, an XRD, and a handheld XRF. These instruments will be discussed in detail in Section 3. Each EVA included three crewmembers: one NASA astronaut and two geologists.

#### **2.3.1.2. Kilbourne Hole, Potrillo Volcanic Field, NM**

The second RIS<sup>4</sup>E field deployment was conducted at the Kilbourne Hole maar volcanic structure in New Mexico (Figure 3). Used as a planetary analog site since the Apollo field training trips, Kilbourne Hole is the largest in a chain of maars that formed from the interaction of near-surface magma and water-saturated ground (Hoffer, 1976; Julian & Zidek, 1991). Four EVAs were conducted in June 2017 to explore the phreatomagmatic and other volcanic deposits at Kilbourne Hole. Three EVAs looked at the layered phreatomagmatic explosive deposits and their interaction with the local basaltic deposits while the fourth EVA examined the mantle xenoliths erupted at the site. The xenoliths are an ideal target for in situ instrumentation as these features examined in context with the fine layering at Kilbourne Hole are challenging to sample but easy to access with handheld instrumentation. The in situ analytical capabilities available to RIS<sup>4</sup>E crewmembers meant that they were able to get contextual data about these features without damaging them. The major science objectives for the four Kilbourne Hole EVAs were to evaluate what the Kilbourne Hole structure was, to determine (if the structure turned out to be volcanic, as the crew did not have confirmation of that prior to the first EVA) what the eruptive history of the region might be, and to evaluate the composition of both the primary features at the structure as well as the xenoliths themselves. The Kilbourne Hole EVAs were conducted by one NASA astronaut and one field geologist to provide both operational and scientific feedback. Instruments available to the crew on these EVAs included LiDAR, an infrared spectral imager, a handheld XRF, and a laser-induced breakdown spectrometer (LIBS), all of which will be discussed in detail in Section 3. Low-altitude remote sensing data were collected independently of the EVAs using an unmanned aerial vehicle (UAV) to provide detailed geology and topography for later assessment of the field site and science objectives (Figure 3).

### **3. Field Portable Instrumentation**

This study was conducted with two different types of instrumentation, each designed to be implemented in one of two different stages of an EVA: 1) site-scanning technologies initiated from the simulated rover parking location (the starting locations for each EVA), and 2) portable instruments to be deployed by the crew during the EVA itself. Below we discuss each technology, any precedent there may be for the technique being deployed on another planetary surface, the procedure for deploying each instrument, and any other operational considerations or constraints involved with the instruments. Instruments used in this study are listed in Table 1 and described below.

#### **3.1. Site Scanning Technologies**

Site scanning instruments can be deployed to provide contextual data for an EVA site. In a Desert RATS-like scenario, the instruments may be mounted on a rover platform, allowing for data collection of a site (Site of

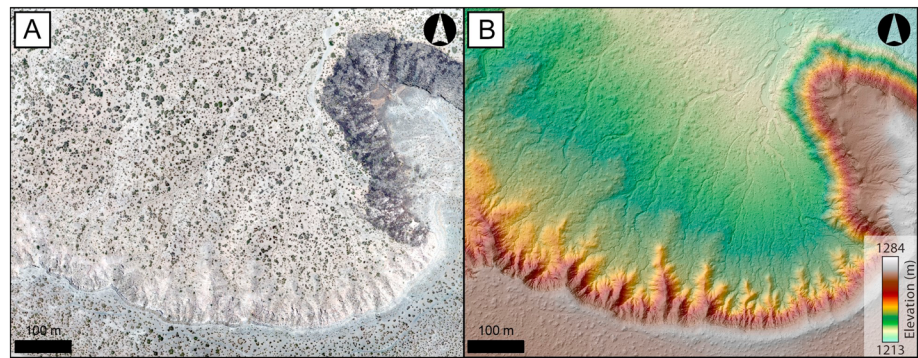


**Figure 3.** The rim of the Kilbourne Hole maar volcanic crater showing the geology and topography for RIS<sup>4</sup>E EVA fieldwork. (a) An orthoimage created from UAV camera data show the pervasive light-toned sediments that mantle most of the area, above and below the crater rim. The rim walls expose a variety of different dark and light layers targeted during the RIS<sup>4</sup>E EVAs, and vegetation cover is sparse. (b) A high-resolution digital terrain model (DTM) shows the smooth plateau (bottom right) and the typical erosion pattern with gullies in crater walls and a dendritic pattern of steams in the crater floor.

Interest, or SOI) as soon as the crew parks next to the SOI. For RIS<sup>4</sup>E EVAs, the crew would approach an SOI on foot, following a track while being cognizant of the MMSEV's capabilities, and select a simulated rover parking spot where they could begin each EVA. As rovers were not used, RIS<sup>4</sup>E simulated EVAs included crews operating the scanning instruments by instructing each instrument team to initialize data collection once the crew chose the simulated rover parking location.

### 3.1.1. Cameras and General Site Context With Audio Notes

Tools used in Desert RATS included a Gigapan camera (a high-resolution panoramic imaging system) mounted on the top of the rover (Young et al., 2013), and correspondingly, RIS<sup>4</sup>E deployments used cameras that were used to document each SOI. Photos were taken by the RIS<sup>4</sup>E crews of sampling locations during the EVA, but prior to rover egress, the crews took context photos of each SOI showing the site with a broad field of view. Additionally, the LiDAR and infrared spectral instruments acquired photographs as part of their data acquisition procedures, which RIS<sup>4</sup>E crews could access as analogs for Gigapan images. The crew took pictures with handheld cameras of the entire outcrop to be sampled upon approach to the site, documenting overall geologic context (or a general description of the site and how it fits into the broader exploration zone) in addition to specific site photos. The crew also took this opportunity to describe the site from their perspective and state the plan for the EVA aloud. Each crewmember wore a chest-mounted GoPro camera that continually recorded audio and video data so these observations were continually captured. The audio and photographic data taken during these steps provided valuable follow-up information for noncrew members to put all other data taken during the EVA into context after the mission.

**Table 1**

*Table Showing All Instruments Used in This Study, What They Measure, and Their Science Value*

Instrument	Measurement	Science value
Cameras (Gigapan, GoPro)	Photographs and Panoramic Images	Site context for field operations and science objectives
Terrestrial Laser Scanning (tripod-mounted LiDAR)	Surface geometry and elevation	
Infrared spectral imaging	Quantitative and qualitative information on surface mineralogy and textures	
Low-altitude remote sensing (kite and UAV)	Photographs and DTM data	
XRF	In situ geochemistry	Real-time data for increased scientific understanding, for decision making, and for sample triage
LIBS	In situ geochemistry	
XRD	In situ mineralogy	

*Note.* LIDAR = light detection and ranging; UAV = unmanned aerial vehicle; XRF = X-ray fluorescence spectrometer; LIBS = laser-induced breakdown spectrometer; XRD = X-ray diffraction.

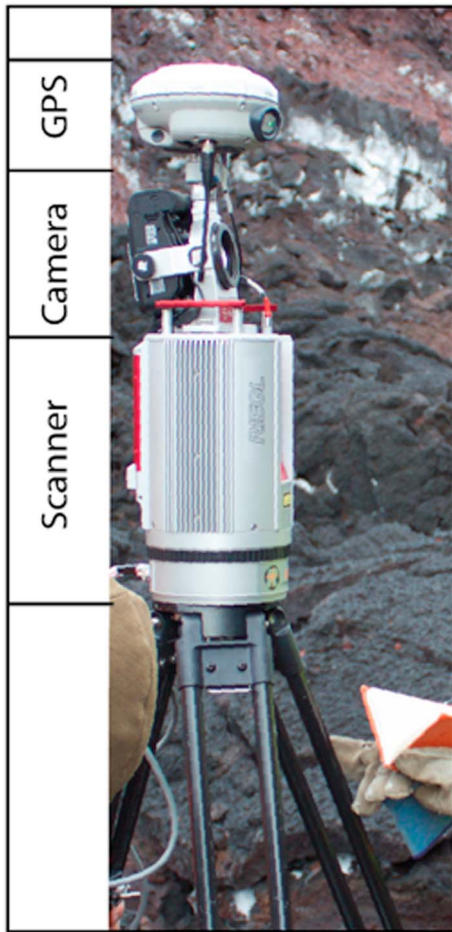


**Figure 4.** After (Whelley, Garry, et al., 2017; Whelley, Scheidt, et al., 2017): TLS field setup. Crews initiated TLS data collection after choosing a simulated rover parking location. TLS data served as a base map for all other data.

### 3.1.2. LiDAR

LiDAR is a method of accurately obtaining surface geometry and elevation by bouncing pulses of light off an interface, detecting their return and precisely measuring the two-way travel time. Developed for military applications, LiDAR is now commonly used in atmospheric studies (e.g., Devara et al., 1995) and geomorphology (e.g., Carter et al., 2001). LiDAR data are also increasingly being used for mapping volcanoes and their eruptive products (e.g., Cashman et al., 2013) by characterizing the intensity of laser returns from lava flows (Mazzarini et al., 2007) or deriving highly accurate digital terrain models (DTMs) of active flows (Favalli et al., 2010) and deposits (e.g., Csatho et al., 2008; Scott et al., 2008). LiDAR observations have also been used to map surface roughness and differentiate lava flow terrains (Morris et al., 2008; Whelley et al., 2014; Whelley, Garry, et al., 2017; Whelley, Scheidt, et al., 2017). Terrestrial Laser Scanning (TLS) is a type of LiDAR scanning, used at each RIS<sup>4</sup>E EVA location that uses a tripod-mounted instrument (Figure 4).

TLS has not been operated on any planet besides Earth. However, topographic data are routinely derived from lander and rover based images using photogrammetry (e.g., Maimone et al., 2004). This process utilizes two or more camera images taken from different positions with a known baseline distance. The observed parallax of objects common to two or more images and the correlation between image pixels are used to triangulate and estimate the distances and positions of objects in the field of view (e.g., Asal et al., 2000; Maimone et al., 2006; Stal et al., 2013, and references therein). Photogrammetry has been augmented with LiDAR data as well (Larsen, 2014; Scheidt et al., 2015; Stal et al., 2013; Whelley, Garry, et al., 2017; Whelley, Scheidt, et al., 2017). For these reasons, future landed and roving spacecraft are likely to carry a combination of camera and LiDAR instruments that provide integrated image and distance data (Chen et al., 2017; Shaukat et al., 2016).

In this study, a Riegl VZ400 (Figure 4) was used during RIS<sup>4</sup>E EVAs as a site-scanning instrument to collect TLS data at each SOI. For each given EVA, a scan was initiated by the RIS<sup>4</sup>E crews from the simulated rover

parking location prior to egress, which would later serve as a base data set on which in situ data could be overlain. The TLS was mounted on a tripod, about 1.5 m tall and approximately 10 m from the EVA location, in the location the crew chose for the simulated rover parking and egress location. Each scan was taken with 0.04° angular spacing, which achieved 7-cm spacing between points 100 m from the scanner. This setting was empirically determined as it is the optimum balance between instrument scanning time and data resolution. The instrument's vertical field of view was 100° and extended 40° below horizontal and 60° above horizontal. A rotating stage enabled data to be collected from all directions. Photographs were taken using a top mounted digital camera that facilitated colorization of the TLS point cloud for context and could also be accessed by the crews in place of the Gigapan images that were available to the Desert RATS crews. A Trimble R8 Global Navigation Satellite System (GNSS) Global Positioning System (GPS) receiver was mounted on top of the camera (Figure 4) to place the scanner and image data in a geographic reference frame.

One additional consideration is that the TLS field of view must be completely free of unwanted obstructions in the scene for the entire duration of the scan. In the RIS<sup>4</sup>E EVA scenario, this implies that the crew should initiate the scan immediately after parking at the site. While they prepared for the EVA and simulated egressing from the rover, the TLS scan could run, requiring no interaction with the crew, so that it was completed by the time the crew were ready to work within the field of view. Once the decision to begin an EVA, and therefore to initiate a LiDAR scan, was made, the setup and scan time was approximately 20 min, although future technological advances are likely to decrease this acquisition time.

### 3.1.3. Infrared Spectral Imaging

Infrared spectral imaging is a passive remote sensing technique that provides quantitative and qualitative information on surface mineralogy and textures. Depending on the wavelength range, spectral resolution and number of spectral channels, infrared spectral imaging can also be used to measure surface and atmospheric temperatures, atmospheric compositional properties, and study transient atmospheric phenomena such as gas plumes or suspended dust. Both near infrared (NIR) and thermal infrared (TIR) spectral imagers have been incorporated in orbital and/or rover missions to the Moon, Mars, and a range of other solar system bodies. From orbit, examples of these include the Thermal Emission Imaging System in orbit around Mars on the Mars Odyssey spacecraft (Christensen et al., 2004), the Observatoire pour la Minéralogie, l'Eau, les Glaces et l'Activité instrument orbiting Mars on the Mars Express spacecraft (Bibring et al., 2005), the Compact Reconnaissance Imaging Spectrometer for Mars on the Mars Reconnaissance Orbiter (Murchie et al., 2007), the Moon Mineralogy Mapper that orbited the Moon on the Chandrayaan-1 spacecraft (Green et al., 2011), the Diviner Lunar Radiometer Experiment orbiting the Moon on the Lunar Reconnaissance Orbiter (Paige et al., 2010), and the Visible and Infrared Mapping Spectrometer that imaged Saturn on the Cassini spacecraft (Brown et al., 2004). From the ground, the Panoramic Camera (Bell et al., 2003) and MastCam (Grotzinger et al., 2012) multispectral near-IR instruments were incorporated into the Mars Exploration Rover (MER) and Mars Science Laboratory (MSL) missions, respectively. Infrared point spectrometers have also been incorporated on numerous orbital and lander/rover missions. Additionally, demonstration of ground-based infrared spectral imaging in terrestrial exploratory studies have recently been progressing (Greenberger et al., 2015; Ramsey & Harris, 2012). For future human exploration of planetary bodies, infrared spectral imaging could be a useful tool for tactical guidance and/or documentation of unit spatial distributions and sample context.

In this work, we deployed two types of TIR spectral imagers: a simulated multispectral frame imager (Figure 5a), measuring five channels with an approximate bandwidth of 0.5–1.0  $\mu\text{m}$ , and a scanning hyperspectral imager (Figure 5b), measuring over 30 channels with a 20  $\text{cm}^{-1}$  spectral resolution. Both instruments sense thermal radiance between approximately 8–13  $\mu\text{m}$  (which captures the major spectral features of silicate geological materials abundantly found at our field sites, and also is a wavelength region where Earth's atmosphere is relatively transparent). The simulated multispectral frame imager used in this work acquires single frame images, with a field of view of roughly  $25 \times 19^\circ$ . The hyperspectral imager used in this work has a vertical field of view of  $9^\circ$  and a user-selectable image width, allowing for panoramic data acquisition.

We simulated a multispectral frame imager by manually placing optical bandpass filters on a lens mount in front of a commercially available thermal camera. The center wavelengths of these filters are 8.3, 8.6, 9.1, 10.3, and 11.3  $\mu\text{m}$  (filter functions shown in Appendix A.1 of Ito et al., 2018), which were chosen to identify silicate minerals by capturing their major spectral features (reststrahlen bands). Five images, one for each filter, were acquired within a time frame of approximately 3 min. An additional image is acquired without filters, bringing the total acquisition time to approximately 3–4 min. Because the filters are outside of the optical path between the detector and internal calibration target, accurate radiometric calibration required external calibration targets (Figure 5a). Typical setup times for the calibration targets and camera were approximately 10–25 min, which included the time spent unloading the targets from backpacks, wiring the targets to data loggers and heater, deciding placement of the targets (based on distance from imager and orientation relative to the imager), allowing the target heater to reach appropriate temperature, and assembly of the tripod and camera. It is important to note that both the simulated multispectral instrument as well as the calibration targets were not commercial products, and thus not as ideally packaged or streamlined as would be expected for a commercial or flight instrument.

The hyperspectral panoramas were acquired using a prototype instrument under development by Spectrum Photonics, Inc. (Figure 5b). Data acquisition times, which included a measurement of an external calibration target to the side of the scene, were approximately 4 min. Setup of the instrument involved assembly of tripod, connection to power source and laptop, and verification of mirror alignments. The duration of these setup activities ranged from 3 to 5 min. The same constraints exist here as with the TLS operation, as ideal data acquisition will not contain people in the images. These data are therefore best collected as part of the initial data collection procedure, initialized by the crew when they initially park the rover at the EVA site. Details about theories, instruments, results, and limitations of infrared spectral imaging and its use in geological field work can be found in Ito et al., this volume.

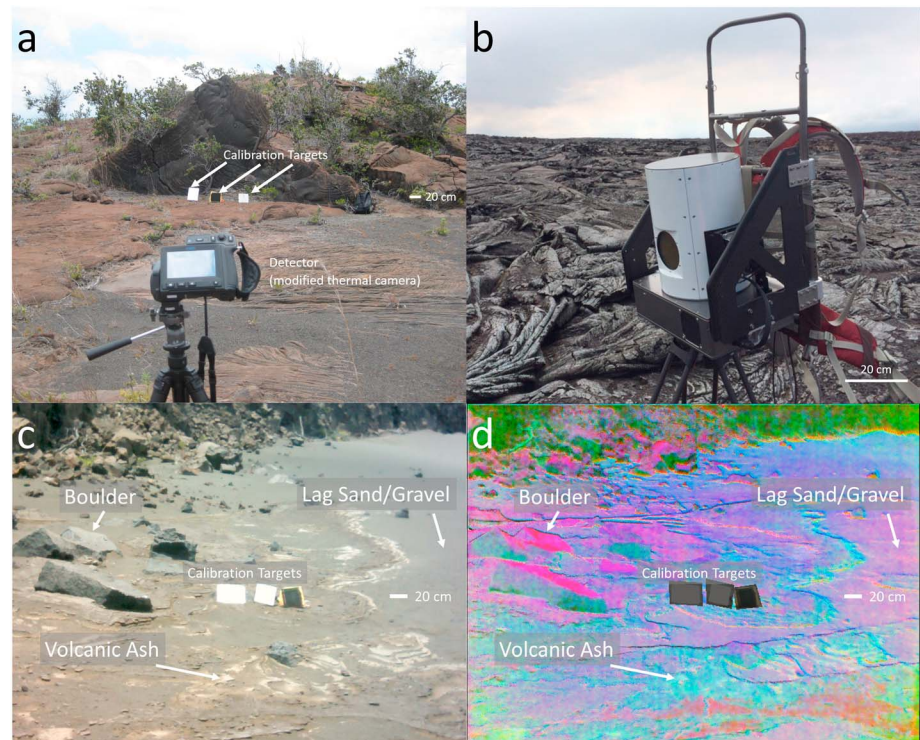


**Figure 5.** (a) A typical setup of multispectral frame imager and external calibration targets in the field. (b) Scanning hyperspectral imager (image credit: Spectrum Photonics, Inc.). (c–d) Example data product from infrared spectral imaging. The scene is at Kilauea field site seen in visible light (c) and false color infrared (d), derived from the multispectral frame imager. Compositional and/or textural variations in the scene are captured.

#### 3.1.4. Low-Altitude Remote Sensing

Although the TLS data provide high-resolution topographic information about each sampling site, we also collected high-resolution aerial images of the site in order to provide a broader overhead field of view of the geologic context for field operations and science objectives. The activity was conducted separately from the EVA to evaluate the technology's potential to add mission value and possible future integration into EVA operations. Several airborne systems have been considered for planetary missions, including helicopters (Novak et al., 2015), airplanes (Levine et al., 2003) and balloons (Greeley et al., 1996). The Mars Helicopter Scout is a robotic helicopter that will help scout science investigation targets and aid navigation for the Mars 2020 rover. This UAV will have a camera for navigation during flights (2–3 min in duration each) and a second camera to collect high spatial resolution color imagery of the martian surface. Our team has employed both kite and UAV borne camera systems in previous NASA-funded studies for terrestrial analog work, such as PGG (Planetary Geology and Geophysics) and mission scenarios to demonstrate the value of low-altitude airborne imaging technologies (SSERVI RIS<sup>4</sup>E). A range of data acquisition scenarios was tested, specifically different aerial platforms and modes of image acquisition.

In the first use case scenario, the addition of a synoptic point of view from a single low-altitude aerial image greatly enhanced operational awareness (Figure 6a). We utilized a kite-tethered aerial camera system with radio-controlled pointing to observe surface conditions and EVA activities. At a slant distance of roughly 50 m, we observed from live video at an off-nadir point of view with high fidelity (effective spatial resolution was about 2 cm per pixel). The radio control allowed camera-pointing adjustments and triggering high spatial resolution still images to focus on the EVA team or points of geological significance. With little time lag or data postprocessing requirements, this capability allows rapid connections between observations on the ground and synoptic information seen from an aerial perspective. For example, the aerial extent of smooth versus rough lava textures can be seen (Figure 6a). This information is sufficient to allow the field team to make adjustments for safe navigation or data collection. The results of this experiment were positive, but the effect of increasing altitude and distance of the camera was not tested here.

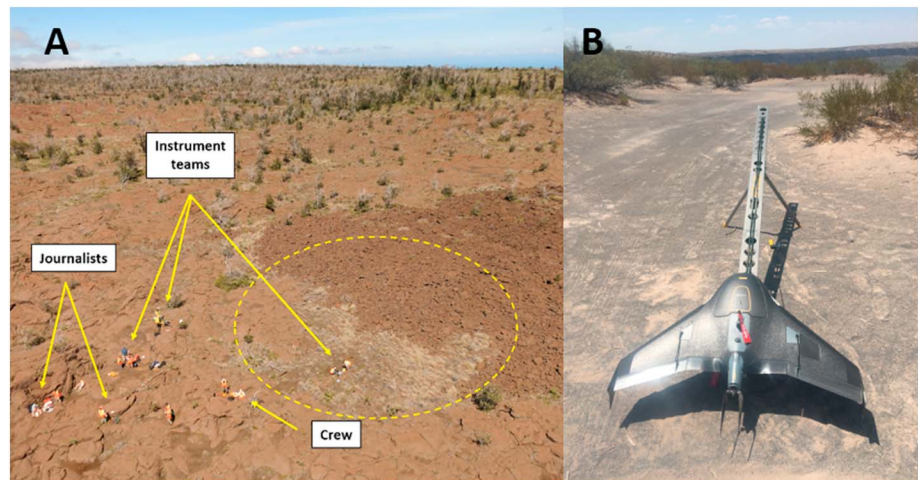


**Figure 6.** (a) Kite-borne image of an EVA site from the D1974 flow, HI, field site showing the RIS<sup>4</sup>E EVA field methodology. The crew is investigating the surface while the instrument teams standby for the crew to request data. Additionally, each RIS<sup>4</sup>E deployment included a team of Science Journalism students from Stony Brook University embedded in the RIS<sup>4</sup>E team to learn about conducting field science and integrating science and human exploration (Jones et al., 2017). (b) The Trimble UX5-HP, a fixed-wing UAV, was deployed at Kilbourne Hole to acquire images and DTM data to provide a broad field of view of the RIS<sup>4</sup>E field site.

In a second use case scenario, advanced capabilities were tested using the aerial image data from both kite and UAV systems. Multiview stereophotogrammetry (MVSP) methods (Scheidt et al., 2015) are capable of generating centimeter to sub centimeter resolution orthoimages and DTM data (Figure 3), where the spatial resolution is dependent on operational parameters such as look angle, imaging altitude, lens focal length and the camera sensor size. Prior to data acquisition, a flight plan is designed to collect aerial images with sufficient overlap (60–80%) to allow for MVSP, typically a grid pattern. Mission planning for UAV missions, and therefore the resource requirements for postprocessing, is highly efficient because the minimum number of images needed to produce a DTM is collected according to a preconfigured flight plan. The orthoimage and DTM of Kilbourne Hole was produced in the weeks following the UAV data collection phase. Utilization of a kite system was different because images were collected based on a timed camera trigger, set to a 3-s interval, resulting in sufficient overlap but an oversampled grid. For both kite and UAV systems, postprocessing and production is time-consuming and requires processing power to develop these science products fully. Although rapid production of low spatial resolution products is possible, the full capability was not practical or tested during EVAs.

In the field, kite and UAV systems have different operational advantages, but they produce equally useful products. For example, images acquired from a kite-borne 10 megapixel resolution camera at an altitude of approximately 60 m were used to create orthoimage data (1.8 cm per pixel) and DTMs (7 cm per pixel) of lava flows at the D1974 lava flow (Scheidt et al., 2015). The resulting raw data, a cloud of three-dimensional points, are comparable in format and quality to TLS data (Scheidt et al., 2015; Whelley, Garry, et al., 2017; Whelley, Scheidt, et al., 2017), which also allowed the production of a fused photogrammetric and TLS data set that accurately represented the ground surface. Approximately 500 m<sup>2</sup> of flat terrain can be surveyed using a kite-borne platform over a period of 1 hr, including setup, take-off and landing of the aerial equipment. Operational constraints of using a kite include the need for fairly consistent and reliable wind direction and speed, necessary to launch and control the imaging system. Although a kite-borne imaging asset would only be relevant in a mission scenario on a planet with an atmosphere, it is unlikely due to its complexity, but should not be ruled out as a low-tech deployable tool pending further technical modifications. A kite-borne system ultimately becomes impractical for area-wide low-altitude remote sensing and mapping for a crewed planetary mission because coverage would likely be achieved by a crewmember on foot, manually translating the camera system around the region of interest.

For RIS<sup>4</sup>E EVAs, these data serve as a simulated mission analog where the expectation is that there would be similar data sets available to mission planners from orbital or other deployable low-altitude remote sensing

assets. For example, the use of a Trimble UX5-HP (Figure 6b), a fixed-wing UAV, was tested at Kilbourne Hole to rapidly acquire data of the crater rim (Figure 3). This system was equipped with a higher resolution camera (Sony a7R) and images were used to produce a 1 cm per pixel orthoimage and DTM data without the use of a time-consuming survey of ground control points using a dGPS (Differential Global Positioning System). The aircraft was launched from a stationary location using a catapult (Figure 6b). A preprogrammed flight guided the aircraft to the region of interest to acquire multiple overlapping images. The aircraft has advanced onboard dGPS and navigation systems that allow the crew to monitor the flight remotely. These systems allow for each 36-megapixel camera image to be oriented in a precise three-dimensional position and orientation and enables the completion of the photogrammetric survey with little manual effort. The aircraft lands automatically at the take-off location, and data are downloaded shortly after for calibration, postprocessing and production of remote sensing orthoimages and DTM data. Although a rigorous investigation of how spatial resolution affects situational awareness for EVA mission has not yet been completed, image data from the UX5-HP in low (15-mm lens, 4 cm per pixel) and high (35 mm lens, 1 cm per pixel) spatial resolution modes give clues to the usefulness of low-altitude UAV image data. Images captured at a lower mode have far less fidelity in identifying individual field crewmembers and specific activities.

### 3.2. In Situ Analytical Technologies

Whereas the instruments discussed above are used upon crew arrival at an SOI to characterize the area from a distance and in general to provide field of view contextual data (and conceivably a base map) for all other data and samples collected during an EVA, the instruments discussed in this section are all capable of providing data in real time to a crewmember during the EVA. These technologies are operated by a crewmember (with varying levels of involvement) and will result in the return of data that can be assimilated and incorporated on an EVA-by-EVA basis. These data can be used both for tactical decision making (or information that is incorporated real time during an EVA that influences how the rest of that EVA is conducted) and for strategic decision making (or information that is incorporated in between different EVAs that influences how the rest of a mission's EVAs are designed and conducted; Hollnagel, 1993; Feigh et al., 2007). Each in situ technology used in this study is discussed here, with an introduction of each instrument, its involvement on any prior planetary missions, and the operational framework used for each instrument for the RIS<sup>4</sup>E study. It should be noted that the crewmembers were entirely responsible for selecting a location where in situ data would be obtained. These decisions were based entirely on the crewmember's preferences about what they wanted to determine about their exploration zone. For example, in some cases, a crewmember just wanted a comprehensive in situ picture of the geochemical diversity at a site, meaning that they would request an in situ measurement at each new rock unit they delineated in the field. In other cases, they wanted to understand if there were differences between one sample or outcrop encountered in the field and a previous sample, which at times impacted their sampling decisions. These decisions were based also on the EVA objectives for each site, which are described above.

#### 3.2.1. hXRF

Laboratory XRF is a well-established and frequently used technique in obtaining diagnostic compositional data on geological samples (Beckhoff et al., 2006; von Hevesy, 1932; Jenkins et al., 1995; Jenkins, 1999; Norrish & Hutton, 1969; Norrish & Chappell, 1977; Parrish, 1956; Shaw, 1952; etc.). Recently, developments in x-ray tube and detector technologies have resulted in miniaturized, field-portable instruments that enable new applications. Several companies (i.e., ThermoScientific, Bruker, and Olympus) have led the way in developing handheld XRF (hXRF) analyzers for use in industrial, commercial, and scientific applications (e.g., Shrivastava et al., 2005; Markey et al., 2008; Margui et al., 2012; among many others). All RIS<sup>4</sup>E work uses an Olympus Innov-X DELTA Premium Handheld XRF Analyzer. Weighing roughly two kilograms, the instrument is equipped with a rechargeable Li-ion battery, a large-area silicon drift detector (with a resolution of approximately 145 eV), and a 4 W Rh anode X-ray tube that provides the excitation source. The x-ray tube geometry and variable excitation source (ranging from 10 to 40 keV) configurations allows for the analysis of a large range of the periodic table. The hXRF used in this study is capable of analyzing elements Mg and heavier, though the major elements (Mg, Al, Si, P, K, Ca, Ti, Mn, and Fe) were the focus of this study due to the robust calibration curves determined in Young et al. (2016). Additional work is in progress now to develop robust calibration curves for the majority of the elements that the hXRF is able to detect. While traditionally used in industry and mining as well as the archeological applications referenced above, the hXRF has more

recently been calibrated for use in geologic settings and is beginning to be integrated into analog missions for planetary surface exploration (Young et al., 2011, 2012, 2014, 2015, 2016).

There is precedent for deploying similar in situ analyzers on other planetary surfaces as four martian rovers (Pathfinder, MER Spirit and Opportunity, and MSL Curiosity) have operated or are currently operating Alpha Particle X-Ray Spectrometers (APXS; Rieder et al., 1997, 2003; Gellert et al., 2009). The APXS measurements made on the surface of Mars have been crucial in documenting and understanding the in situ chemistry at each landing site and fitting this chemistry in to a broader geologic context (or how each analysis location fits into the geologic history of the exploration zone as a whole). In addition to the numerous scientific contributions that the APXS measurements have contributed to (e.g., Ming et al., 2006; Squyres et al., 2004; Squyres et al., 2008), one major operational advantage of the instrument is its ability to provide rapid (relative to laboratory analyses) compositional information about all sampling sites and traverse locations. Though the most robust data come from lengthy, several-hours-long collection times, the instrument is also capable of shorter integrations when a quicker compositional look is warranted (Rieder et al., 1997). This philosophy of quicker, snapshot views of a sample of interest as compared to more robust, longer integrations is a crucial one, and it will be discussed later in this paper.

Whereas APXS technology has been deployed on several robotic platforms, this RIS<sup>4</sup>E effort describes the use of a similar technology, hXRF, in crewed planetary surface exploration. The deployment procedure used during RIS<sup>4</sup>E EVAs is discussed here.

1. The crew decides on hXRF sampling sites of interest while conducting an EVA. These decisions are based on understanding the geologic history of the SOI, determining high priority sampling locations, and answering more detailed, site-specific scientific questions that may arise depending on the chosen EVA location.
2. Depending on the scientific question that the crew seeks to answer, minimal sample preparation is completed. For example, if the crew wants to understand the chemistry of a fresh sample unobscured by weathering products, they use a tool (i.e., a rock hammer or rock abrasion tool) to create a fresh sampling surface. If the crew instead wants to interrogate the natural surface (e.g., a weathering rind), no or very minimal sample preparation is necessary.
3. The crew places the nose cone of the hXRF on the site of interest (Figure 8a). In this case, the instrument window is 8 mm on a side, meaning that the analyzer will give the user the composition of that area on the sample. Care must be taken when placing the instrument on the sample to ensure the correct 8 mm × 8 mm area is being analyzed. Flat, homogenous surfaces are best suited for data collection.
4. The current integration, or analysis, time for the commercial XRF analyzer is 60 s. This integration time was determined empirically by Young et al. (2016) as appropriate for relevant analog terrains with the current Olympus model. It should be noted that future instruments under development may bring this integration time to less than 60 s, in which case all timeline information presented here can be easily amended. This study takes only one 60-s measurement per spot, as this was also empirically determined to be representative of the bulk chemistry of each analyzed location.
5. After integration is complete, the crew removes the analyzer from the sample. The crew will then photo document the precise location of the analyzed spot as well as broader field of view images showing where the analyzed spot sits in context with the EVA site or outcrop as a whole. If only one crewmember is present, they can point at the spot (to show the precise analysis area) and take a photo. If at least two crewmembers are present (as was the case for RIS<sup>4</sup>E EVAs), the first crewmember can spend the 60 s of analysis time holding the hXRF in place while the second crewmember can photo document the site during the same 60 s.
6. After analysis and photography, documentation is required noting the instrument analysis number, image number, and any associated descriptions (i.e., site description or rationale for the analysis). Though a field book was used in the RIS<sup>4</sup>E deployments, voice documentation (either to an IV crewmember located nearby or via an onboard recording device) is preferable in a planetary exploration setting. This is the technique used in Desert RATS and is likely how astronauts will document field sites in the future.

All of the steps described above yielded a total data acquisition time for one sampling spot of 2 min. Again, should the instrument integration time decrease through future technology advancements, this total time would directly reflect that change.

### 3.2.2. Laser-Induced Breakdown Spectroscopy

The use of laser-induced breakdown spectroscopy (LIBS) on planetary bodies, specifically Mars, has been well documented and proven as a highly useful addition to rover payloads (e.g., Blaney et al., 2014; Clegg et al., 2014; Graff et al., 2011; Maurice et al., 2016; Meslin et al., 2013; Nachon et al., 2014; Ollila et al., 2013; Schröder et al., 2015; Wiens et al., 2012). Additionally, laboratory work continues to demonstrate the usefulness of this technique under Mars-like conditions (e.g., Boucher et al., 2015; Dyar et al., 2011, 2012). This study uses a field portable SciAps Z-300 Handheld LIBS Analyzer to assess the elemental chemistry of materials at each EVA location at the Potrillo Volcanic Field. Similar to the hXRF, the LIBS weighs approximately 4 pounds (2 kg) and uses a rechargeable Li-ion battery. It includes two stacked high-resolution spectrometers that together span a spectral range from 190 to 950 nm to identify elements from H to U, though the detection limits vary depending on the element. The instrument emits a 1,064-nm laser pulse to ablate a small volume of sample that generates a plasma plume. Each analysis occurs in the presence of an automated Ar purge deployed in front of the analyzer; this improves line intensity compared to operation in atmosphere. The Ar purge is used to provide an inert atmosphere in which the plasma can be analyzed. Optimal Ar pressure is 12–14 psi, and the Ar tanks are changed out in the instrument when the pressure drops below 12 psi. This aids in the quantification of the data as it improves precision and detection limits. An integrated camera allows the user to see the area that will be laser. These analyses provide geochemical information to help address in-field science questions, as well as serve as a way to visually triage interesting samples to high grade for further laboratory analyses.

The use of the handheld LIBS is complementary to hXRF analyses in that LIBS allows for the quantification of several light elements that are not possible to detect with hXRF (e.g., H, C, N, and O). Specifically, the Limit of Detection (LOD) for these elements are as follows: LOD for H < 0.1 wt.%; LOD for C = 0.1–0.2 wt. % under optimal conditions; LOD for N > 0.5–1.0 wt.%; LOD for O = 1–5 wt.%. Though these LODs are well established for alloy samples, as the LIBS is primarily used in metal and alloy quality control work, there are additional efforts currently underway to refine these LODs for geological samples. While XRF provides quantitative measurements of most elements, and element identification is based on detection of intensity at well-understood and straightforward fluoresced wavelengths, the LIBS relies on detection of element spectral lines and calibration curves developed using standards to determine quantitative abundances of elements. The handheld LIBS cannot currently quantitatively analyze loose powders and/or sediments as the laser shot will disperse the powder and greatly reduce the accuracy of the geochemical analysis, but some work on optimizing these analyzes is ongoing. XRF, however, can analyze loose sediments, something done in several locations by the EVA crews (in these terrestrial field deployments loose sediments can be sampled and pressed into pellets for LIBS analyses in the laboratory at a later date if these data are desired and time allows). The LIBS has two pre-programmed raster grids of laser points for a given sample area, 3 × 4 and 16 × 16 (each laser point in a raster has a spot size of approximately 50 μm). Those individual laser spots are averaged together and both the average elemental composition and the spectra are reported in real time on the LIBS display. We acquire three rasters, where each raster is a 3 × 4 grid (resulting in 12 individual pulse locations, where there are 2 cleaning pulse shots and 3 data pulse shots), for a total of 60 individual pulses. A wavelength calibration is done every 30–40 shots and the calibration is done on the internal stainless steel plate. Even for the largest raster, the total area of the sample assessed is smaller than the XRF spot size (approximately 2.5 × 3 mm, not hitting the material in between the spots in that analysis area; Figure 7). Typical analyses are for bulk chemistry of the desired sample; in this case, three closely spaced areas are measured and the chemistry of those averaged to represent a given sample measurement. This results in an area not the same as, but more comparable, to the area assessed by the hXRF, than is enabled by a single raster area measurement. Additionally, the LIBS has a camera that allows the user to identify the specific sample location for which they want to acquire data. In this study, the viewfinder was used to select a location representative of the bulk rock to ensure that the three shots analyzed by the LIBS is comparable to the bulk composition obtained by the XRF. A benefit of this LIBS capability is that the user can also select individual phenocrysts for analysis. These should not be directly compared to bulk XRF analyses but can be used as an additional data set. This study, however, focuses only on analyses comparable to those obtained by the XRF. Some scientific questions and analyses benefit from chemical analysis of the smaller LIBS spot area. For example, if differences in the chemistry of small-scale features such as veins or particular grains are desired, these can be targeted in one analysis given the small spot size of the LIBS (Figure 8).



**Figure 7.** The pits created by the laser shots from the LIBS instrument are visible here (at tips of arrows). The pits are in a  $3 \times 4$  raster in the blue- and yellow-coated surface of the D1974 lava flow.

The operational framework is similar to that for the hXRF that was described in the previous section with the following differences:

1. The LIBS window must be placed flat on the desired sample spot in order for the laser to fire all shots. If the window is not fully covered or if the LIBS is moved during the analysis then the laser will cease firing and the sample will need to be reanalyzed. The integrated camera can be used to identify the specific sampling location, indicated by a red box in the viewing window. Three analyses were acquired for each sample of interest.
2. The integration time for the commercial LIBS is approximately 30 s for a raster of  $3 \times 4$  (as long as the laser does not misfire as described above). Thirty seconds was determined because, even though the actual data collection takes only a couple of seconds, extra time is required to find an optimal position with the instrument for data collection so the LIBS does not misfire.

The total data acquisition time for one sampling spot including notes and photographs as described in the previous section is less than 2 min, comparable to the hXRF. We used and recommend using the hXRF first, as this instrument is non-destructive to the sample. The LIBS should be deployed second on the same location as the hXRF, using the viewfinder as mentioned above to find representative locations. If additional data is collected (i.e., XRD, VNIR), then it should be collected a few centimeters away from the hXRF/LIBS sampling location to avoid sampling where the mineralogy may have been altered as a result of the LIBS sampling.

### 3.2.3. X-Ray Diffraction

A field portable X-ray diffraction (XRD) was deployed only at the Kilauea site. XRD is a technique that has been long used to study terrestrial mineralogy. Traditionally, XRD measurements have been limited to laboratory instruments with large masses and spatial footprints with substantial power requirements, and oftentimes require specialized sample preparation. However, miniaturized X-ray sources and detector technologies, and a novel sample cell design that allows diffraction measurements in a compact transmission geometry have since been developed. These improvements enabled an XRD instrument, the Chemistry and Mineralogy (CheMin) instrument, to be incorporated into a flight payload for the first time, on the MSL Curiosity rover (Blake et al., 2012). CheMin is tasked with investigating the mineralogy and chemistry of selected rocks and sediments encountered by Curiosity, and was instrumental in the discoveries of Fe-



**Figure 8.** The field portable instrumentation available to the RIS<sup>4</sup>E crewmembers for in situ chemical and mineralogical analyses are shown. (a) The XRF spectrometer is handheld and acquires geochemical data with a 60-s data collection time. (b) The LIBS instrument is also handheld and provides data on the same time scales as the hXRF. (c) The XRD provides both mineralogy and chemistry information after longer integration times and some sample preparation.

saponite and akaganéite in the Yellowknife Bay mudstone (Vaniman et al., 2014), 2:1 phyllosilicates, hematite and jarosite in the lower section of the Murray Formation (Rampe et al., 2017), and tridymite and opaline silica upsection in the Murray Formation (Morris et al., 2016). The success of the Curiosity CheMin analyses prompted the use of comparable field XRD analyses in our study. We deployed an Olympus Terra field portable X-ray diffractometer (with CheMin-like sample geometry, detector, and X-ray tube) in the field to investigate local mineralogy. The Terra instrument weighs approximately 14.5 kg, is housed in a compact rugged case the size of a large briefcase and is powered by rechargeable Li-ion batteries. It incorporates a miniaturized 10 W, 30 kV X-ray tube (Co  $K\alpha$  radiation) and a 2-D Peltier-cooled charge-coupled device. The unique sample vibration chamber requires small sample masses (approximately 20 mg) and mitigates any preferred orientation effects in patterns. Standard patterns have a  $2\theta$  range of 5–55°, and  $2\theta$  resolution of 0.25° full width at half maximum (FWHM). In addition, the detector has energy discrimination capability that reduces background from scatter and fluorescence and also allows some semiquantitative XRF data on elemental chemistry from elements Ca-U. These data can be helpful in constraining the mineralogy of samples and can be compared to the more quantitative XRF data obtained through hXRF analysis. The operational procedures for collecting data using the Terra XRD were as follows:

1. Select a sample for XRD analysis. Sample selection philosophies will be discussed in greater detail in section 4.
2. Samples must be prepared with a particle size of  $<150\ \mu\text{m}$ . For RIS<sup>4</sup>E analyses, we used a mortar and pestle or dremel drill to grind or powder the sample, then sieved the resulting powder to  $<150\ \mu\text{m}$  before loading the powder into the sample cell. Depending on the hardness of the sample, crushing/dremeling the sample can take up to 5 min and loading the sample cell can take up to 2 min.
3. Sample integration time for the XRD is variable. Depending on the complexity of the sample (number and crystallinity of sample components) and the quality of data needed, a crewmember may choose to integrate for only a few minutes (for good quality data from single minerals or simple mineral mixtures) or for as long as a couple of hours (for very high-quality data of more complex samples). The pattern is updated in real time in the software with each exposure, so after a few minutes of integration time (generally less than 3 min), it is possible to determine if the sample is relatively simple or complex. In the case of a complex sample, 30 min integration was found to usually be a reasonable compromise between data quality and time. In terms of data quality, we reiterate that the mission scenario under consideration here involves using instrumentation to gain an increased real-time understanding of the chemistry and mineralogy of a site and to high-grade samples for follow-up laboratory analyses. The goal is not to replace the need for more robust laboratory analyses.
4. As the data acquisition continues the pattern becomes more refined, and the crew can start to understand and assimilate the mineralogy of the sample. The analysis can be saved and interpreted (by the crew or any available science backroom support from Earth) in real time at any point during the integration session.

As instrument operation times vary, it is especially important to appreciate what type of information the XRD can provide to better understand how this instrument fits in to the overall mission architecture. Lessons learned for integrating XRD with XRF analysis are discussed in section 4.

## 4. EVA Timeline Results

During all field EVA operations, detailed timeline data were kept for all steps in each instrument's deployment procedure, including instrument setup, instrument operation initiated, instrument operation concluded, and number of people requires to operate the instrument.

### 4.1. Timeline Evaluation of Selected Instrumentation

Because we sought to isolate instrument operations from a baseline of previously determined EVA timelines with no detailed instrument analysis, we started with an Apollo- or Desert RATS-like EVA plan, with a limited time for each EVA. The baseline operational procedure was that the crew would approach an EVA target on foot, simulating that they were in a rover. They would "park" some distance away from the outcrop. This distance varied by target but typically ranged anywhere from 10 to 20 m from the outcrop itself, based on local terrain conditions. The crew then indicated that TLS and infrared spectral imaging should be initiated. This initialization process did not involve appreciable time added to the timeline, as this would

**Table 2**  
(Above): Total Instrument Operations Times, in Minutes

	D1974 flow, HI			Kilbourne Hole, NM			
	D1974 1	D1974 2	D1974 3	KH 1	KH 2	KH 3	KH 4
TLS	20	19	23	13	22	16	—
Multispectral imager	24	36	18	—	—	—	—
Scanning hyperspectral imager	—	—	—	16 (3)	14 (1)	28 (2)	—
XRF	20 (10)	14 (7)	20 (10)	21 (11)	36 (18)	34 (13)	43 (17)
XRD	0	30 (1)	0	—	—	—	—
LIBS	—	—	—	16 (11)	52 (21)	4 (2)	0
Crew time	69	50	74	60	55	59	62
Total EVA duration	89	94	94	97	143	97	105
Percentage of Total EVA							
Crew Exploration	77.53	53.19	78.72	61.86	38.46	60.82	59.05
XRF	22.47	14.89	21.28	21.65	25.17	35.05	40.95
XRD	—	31.91	—	—	—	—	—
LIBS	—	—	—	16.49	36.36	4.12	—

Note. Total EVA time includes the baseline crew EVA timeline as well as any XRF, LIBS, and XRD instrument operations. For the XRF, LIBS, and XRD, the number of analyses are included in the (#) next to the total analysis times in Table 1. TLS and infrared spectral imaging are not included in the total EVA timeline as these data are acquired before the crew simulated rover egress.

likely be an automatic step in the procedure. Even in the case of the crew having to interact with this more automated field-of-view instrumentation, this time would not count against EVA time as these steps would be completed from inside the rover. The crew would then photograph the outcrop from the parking spot while they conferred together to develop an EVA plan, which also would have taken place prior to egress from the rover so did not count against the EVA timeline. Each EVA was conducted similar to Apollo, with a primary goal of observing the site’s geology and collecting representative samples (e.g., a general exploration of a previously unvisited location, which would likely differ from a previously visited location for which more detailed scientific goals would be developed). As the EVA progressed, the crew identified locations for in situ analyses with the XRF, LIBS, and/or XRD. The crew then announced which analysis was requested and precisely where they wanted it, and the XRF, LIBS, or XRD team moved in to complete the measurements while the crew moved on with their EVA procedure. After finishing working in the site of interest, the crew would return to the starting location and “ingress” the rover. This process is shown here:

Due to the crew working independently from the instrument teams, they were therefore unencumbered by instrument operations and were able to complete a nominal EVA with a nearly identical approach and time limit to those conducted during Desert RATS, while the instrument teams operated concurrently. In this way, we were able to assess the true effect of currently available instrument technologies on a nominal Desert RATS-like EVA timeline. Also, note that the first field site included XRD and XRF while the second field site had LIBS and XRF. It should be noted that no differences were noted in efficiency (or the time it took each crew to determine sampling locations) during the EVAs at Kilauea versus Kilbourne Hole, regardless of the fact that the LIBS was only available at Kilbourne Hole. Detailed timeline data were recorded at each stage of the process, including for each individual instrument team, which allowed us to isolate, for example, how long an EVA would take with and without XRF analyses. Table 2 highlights the amount of time it took to operate each instrument. Note that low-altitude remote sensing data are not included in Table 2 as it is not likely that a kite will be deployed in a relevant mission simulation. These data were collected solely to show the benefit of high-resolution contextual aerial data. More work is needed to investigate this technology and how adaptations might fit in to the mission scenario discussed here.

Table 2, in addition to highlighting the total data acquisition times for each instrument (in minutes), for the crew exploration time, and for the total EVA times, also shows the percentage of crew time taken by observations and sampling, by XRF and LIBS analysis, and by any XRD work completed during the EVA. Had the crew been completing XRF and LIBS work (instead of each instrument team), they would have spent between about 14–41% of their time collecting and documenting XRF data. On EVAs where no XRD or LIBS data were collected, that left >59% of their time to explore the site and collect samples. However,

when an XRD analysis was completed, they had about 53% of the EVA to complete these Apollo-like observing and sampling steps. During the three EVAs where LIBS data were collected, the number of analyses requested by the crew (and therefore the time spent on data collection) varied dramatically from EVA to EVA based on the scientific hypotheses being developed at each site. The second Kilbourne Hole EVA included the most LIBS data (where the crew spent approximately 36% of the total EVA duration on LIBS) which was likely due to the fact that the crew was targeting lighter elements on this EVA, which is a strength of LIBS over XRF. It should also be noted that, due to extremely high local temperatures at Kilbourne Hole, the LIBS instrument overheated and could not be used for the majority of the third KH EVA and the entire fourth KH EVA.

When considering the total number of XRF and LIBS analyses requested by the crew across one field site, we must also consider the scientific objective of that site. For example, on EVAs KH2 and KH4, the crew discovered that these sites were dominated by smaller scale geologic processes (e.g., high concentration of xenoliths at KH4). Alternatively, EVA sites KH1 and KH3 were discovered to be dominated by larger scale interactions between larger units. KH2 and KH4 resulted in a higher number of XRF measurements because the crew was focused on collecting a large data set covering the smaller-scale features, not exploring broader contextual relationships at an outcrop scale. Future EVA planners should keep this in mind, as EVAs targeting fine scale processes will likely require more time spent using in situ instrumentation.

We note that the sample selected for the XRD analysis during the second EVA at D1974 was chosen by the crew based on a previous hXRF measurement. After identifying a unit that they did not completely understand, the crew requested XRF analyses in several locations and, using these data, selected a sample for which they wanted more detailed mineralogy data. This process of using portable instruments to triage for one another was innovative and effective in the case where instruments with longer integration times (and therefore more of an impact on the EVA timeline) are required. However, besides that one occasion, the crew was reluctant to employ the XRD because of the larger time hit of that technology. Our recommendation is to only use the XRD after using the XRF to select the optimal sample. It is also possible to use other in situ techniques to select samples for the more time-consuming XRD analyses (e.g., multispectral imaging, scanning hyperspectral imaging, LIBS, and Raman). In this case, the crew used hXRF, but all of these techniques could possibly be used in this high-grading capacity. Though not yet commercially available, XRD instruments that operate in a reflection mode more similar to the operation of the XRF and LIBS (not requiring sample preparation such as crushing and sieving) are under development (Arzoumanian et al., 2013; Sarrazin et al., 2017). While a more detailed understanding of the use, and optimal interpretation of data from, these instruments would be needed to understand how they would be best incorporated into an EVA, the utility of the existing field XRD technology suggests they could provide very useful contributions to future EVAs.

It is understanding this trade space, of how much time a crew loses in choosing to make a measurement with an instrument against what science value added it gives to them in the field, that will allow future mission planners to make more informed traverse strategies and, later, “flexecution” (flexible execution of preplanned traverses) decisions (Hodges & Schmitt, 2011; Klein, 2007a, 2007b) during each traverse.

#### 4.2. Real-Time Visualization of Scientific Data

While increased access to a variety of in situ data sets is valuable in providing a greater level of scientific detail to the crew about the exploration zone, the complexities associated with viewing and interacting with these data, especially during an EVA, cannot be underestimated. Depending on the mission architecture, crews will be staying a planetary surface anywhere between days, weeks, and months at a time. Should these crews have access to even one high-resolution instrument (e.g., the LIBS), the volume of data being generated by this technology will quickly become burdensome on an already time-pressed crewmember. Making all data, especially if multiple instruments are available and in the cases where missions involve multiple days' worth of EVAs, accessible in a relatively simple layout to a spacesuit-clad crewmember is vital in ensuring that these data will be able to be integrated into traverse planning mid-EVA and mid-mission. To this end, we have implemented the Cue Card system, initially developed for the NEEMO missions (Graff et al., 2017; Young et al., 2018). Cue Cards are a series of files made available to the NEEMO and RIS<sup>4</sup>E crews during EVA (Figure 9). During NEEMO, these Cue Cards were housed on an underwater iDive (a waterproof iPad). During RIS<sup>4</sup>E work, the crew at Kilbourne Hole had access to them on an iPad during each EVA. Cue Cards contained each day's

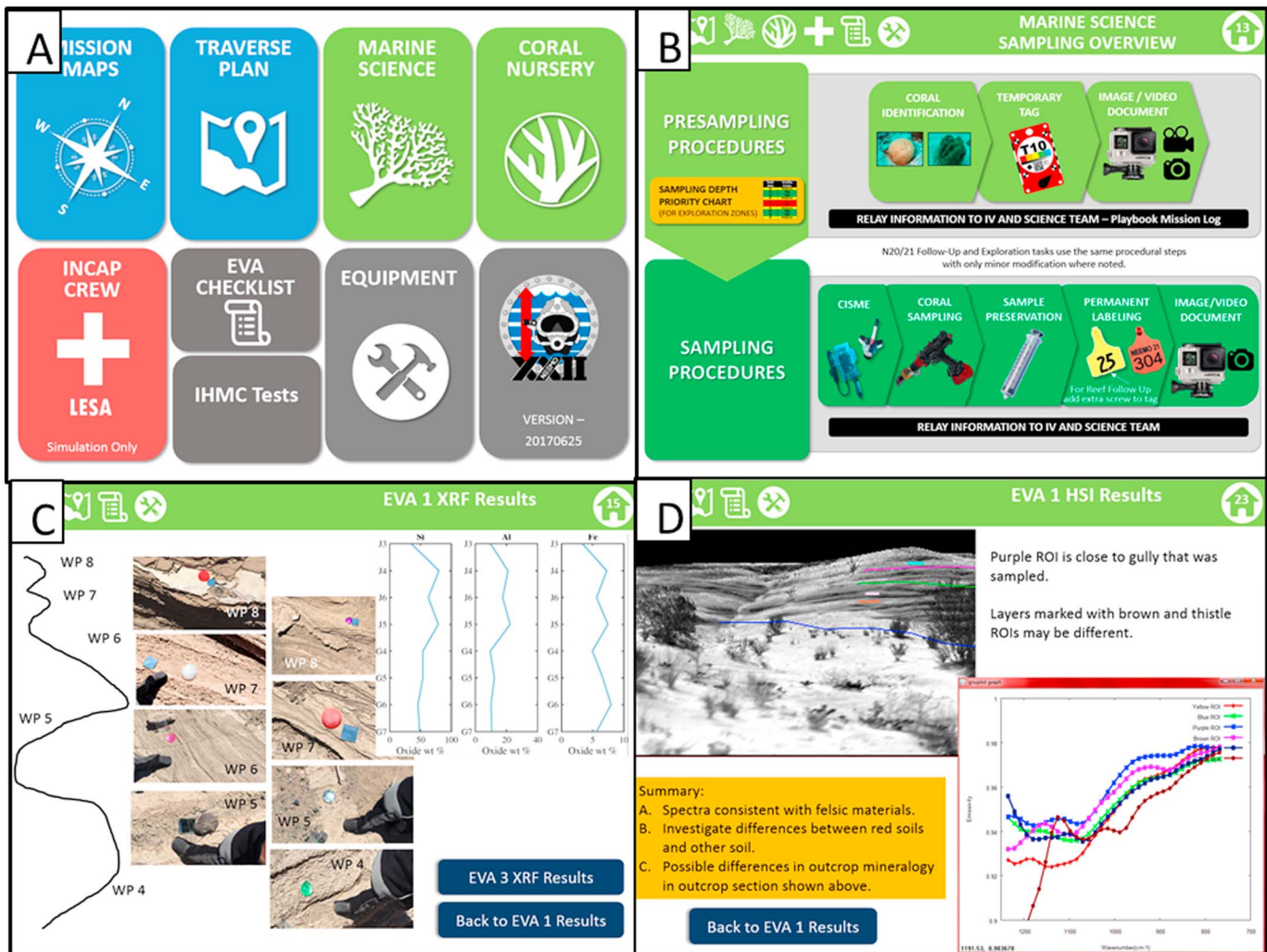


**Figure 9.** Cue Cards used in both NEEMO and RIS<sup>4</sup>E. (a) The home page of the NEEMO Cue Cards. By interacting with the Cue Cards on the underwater iPad, the crew was able to flip through 90 pages of traverse maps, EVA science procedures and sampling tips, troubleshooting procedures, etc. during each EVA. (b) An example of a NEEMO Cue Card showing Sampling Procedures for the NEEMO 22 mission. (c–d) Two 2017 RIS<sup>4</sup>E Kilbourne Hole Cue Cards. Modeled after the NEEMO Cue Cards (Graff et al., 2017), the RIS<sup>4</sup>E Cue Cards showed portable instrument data collected during each EVA. (c) shows hXRF data while (d) shows results from the Hyperspectral Imager.

traverse plan, procedures for sampling and instrument deployment, troubleshooting procedures in the event of instrument malfunction, and each day's instrument data as they are collected. Science support teams could integrate this Cue Card file daily and push it to the crew's iPads to update any instrument data files or to add troubleshooting procedures should issues arise. Having such extensive access to procedures and data increases the degree to which planetary surface crews can operate autonomously from Earth-based science support teams, which is especially important in missions with long time delays (i.e., Mars missions). NEEMO and RIS<sup>4</sup>E EVAs both demonstrated the value in having real-time access to the information provided in the Cue Cards, and future analog missions and planning for future planetary surface missions should incorporate a comparable technology. One way in which informatics like the Cue Cards could be incorporated into future missions is with a heads-up display (HUD) capability. By projecting informatics such as procedures, sampling guidance, and instrument data onto the interior of a spacesuit helmet in an augmented reality platform (where the crewmember can still see their surroundings, but the information is displayed on top of the landscape visible through the helmet), crews will have access to the information without it interfering with their vision. Future technology development should consider this as a solution for viewing instrument data.

## 5. Conclusions and Future Work

It is often the case that terrestrial field scientists wish for more data real-time while doing fieldwork, and it is thought that the same will be true for astronauts exploring other planets. However, the utility of any field portable instrument on a planetary surface mission is still an open question relative to the overall gain in efficiency and scientific return. This question will likely not be fully answered until we are ready to plan a mission to the lunar or martian surface that has defined science objectives. The work outlined here highlights the need for a thorough understanding of the impact of instrument operations on EVA planning because, despite the apparent value of the scientific data collected with current portable technologies, there is a significant impact on the timeline, with approximately 40% of the EVA in some cases being devoted to these instrument operations. While it is not the intention of this work to specifically investigate the scientific value of field portable instrumentation (for an example of the science return possible with some of these instruments, please see Whelley, Garry, et al., 2017; Whelley, Scheidt, et al., 2017; Yant et al., 2018), future work should focus on this crucial issue. It is the belief of these authors that metrics that seek to quantify science return do not adequately capture the complexities of evaluating the utility of field portable instruments and can often be subjective, so future work should center on qualitative techniques of evaluating each technology.

The significant timeline investment required in deploying portable instruments highlights the need for efficient designs in both instrument hardware and software. On one of the RIS<sup>4</sup>E EVAs for example, 18 XRF analyses were requested. The hardware design of flight hardened portable XRF units must both minimize integration time as well as maximize efficiencies for a crewmember in a pressurized spacesuit to operate the hardware. One way to minimize the physical effort that a crewmember must expend in order to hold still during longer integration times (necessary so the XRF and LIBS do not lose direct contact with the sample) is to design the instrument so that it can be used in both handheld and stationary modes. For samples that are able to be isolated from the outcrop of interest (where doing so will not lose geologic context in cases of finer-scaled features), the crewmember could isolate the sample and present it to the instrument, removing the need to position their body to hold an instrument still for longer periods; this method was used for LIBS data acquisition during these EVAs and proved useful. Should the mission architecture include a robotic assistant to the crew during EVA, more development is needed to determine how much crew time will be required to set up, start and stop, and possible repair and/or clean each instrument. With respect to cleaning portable instrumentation, future hardware design might look at active or passive dust rejection by exterior, sensor, or optical surfaces.

Instrument user interface and software design is just as important as the hardware design. If the crew is to incorporate recently collected data and be able to react to it (decide on sampling priorities, flexecute changes to the traverse plan, etc.), they must be able to rapidly assimilate the data in a display that does not overwhelm them with scientific detail in an operational environment where their first priority must be on safety (monitoring consumables, timeline, etc.). We recommend that teams designing future flight instruments focus not only on designing simple yet effective instrument display capabilities but also consider in what mode they want their data displayed (graphical format, ability to display and compare data from multiple EVAs, etc.).

In addition to data visualization considerations, the data processing time and data quality required to make more informed decisions must also be considered. For instance, the LiDAR and multi/hyperspectral cameras can provide detailed, quantified information for a scientist. However, a crew member about to go EVA might only need to know that two rock types are considered different enough to warrant consideration for sampling. Furthermore, recognizing which rocks at a current location are similar to or different from rocks at prior locations within certain limits could be useful. In other words, although all scientific instruments have an ability to provide detailed quantified data, they also present an ability to provide qualitative inferences with much less data processing. Questions to be asked for future instrument development are (1) how accurate is “good enough” for a crew member to make an informed choice relative to a crew member lacking those data, (2) how quickly can data be processed to enable those decisions and can that processing be automated, and (3) where does that data processing occur, in the instrument, in wearable suit computers, onboard a rover, habitat or spacecraft, or back at Earth? While instruments such as the LiDAR and multi/hyperspectral cameras can collect data quickly prior to an EVA, it is important to understand how much time those

instruments might have during EVA preparations to provide a “good enough” data product, recognizing that those data will undergo further data processing later. It is for reasons such as these that instrument testing such as is presented here must be done in a complementary manner to the larger integrated technology tests that evaluate overall architecture design.

Designing instrumentation for human spaceflight (rather than for rover or lander missions or for use terrestrially) must consider the effects of operating those technologies in a pressurized spacesuit in an environment where time is one of the most critical scientific resources of a surface mission. EVAs are highly time limited, which means that every instrument analysis point acquired further decreases the time spent exploring additional locations in the exploration zone, so instrument efficiency is crucial from a design standpoint. As a scientific community, we have the potential to use field portable technologies to increase the science return of a surface mission and influence the quality of samples being returned for detailed laboratory analysis. While these portable instruments will never replace high-precision, comprehensive laboratory work, sample collection can be positively influenced by technologies that support sample high grading.

Finally, we advocate for extensive continued field deployment of in situ instrumentation in a variety of relevant analog environments. Deployment in analog geologic environments enables the study of the combination of technologies that will best provide crews with the maximum variety in scientific data sets while deployment of comparable technologies in extreme environments like NEEMO enable a higher fidelity study of operational concepts for design of future mission architectures and exploration technologies.

#### Acknowledgments

This work was supported by the RIS<sup>4</sup>E node of NASA's Solar System Exploration Research Virtual Institute (T. D. Glotch, PI). Fieldwork was completed under the United States Department of the Interior National Park Service Permit HAVO-2016-SCI-0005. We gratefully acknowledge the field and data processing support of Spectrum Photonics, and specifically Byron Wolfe, Daniel Piquero, Paul Lucey, John Hinrichs, and Casey Honniball. Thanks also to the University of Texas, El Paso Geological Sciences Department for providing us with enthusiastic students for field support as well as space in the department for data processing during field campaigns. We also thank field team support members who provided crucial help in the field including Jacob Richardson, Dean Eppler, Debra Hurwitz Needham, Paul Niles, Kevin Lewis, and many others. We also acknowledge Matthew Miller for his helpful dialogue in the preparation of this paper. Finally, thanks go to two anonymous reviewers for their thoughtful comments which helped to improve the quality of this paper. Because there are no traditional data repositories with which to archive instrument protocols and procedures, the authors will maintain all the data contained in this manuscript for 5+ years. Anyone wishing to access anything discussed in this paper should contact the lead author.

#### References

- Abercromby, A. F. J., Chappell, S. P., & Gernhardt, M. L. (2013). Desert RATS 2011: Human and robotic exploration of near-Earth asteroids. *Acta Astronautica*, 91, 34–48. <https://doi.org/10.1016/j.actaastro.2013.05.002>
- Allton, J. H. (1989). Catalog of Apollo lunar surface geological sampling tools and containers. [Available at <http://cosmochemists.igpp.ucla.edu/Allton-1989-Lunar%20Sample%20Tool%20Catalog.pdf>.]
- Arzoumanian, Z., J. E. Bleacher, K. Gendreau, A. McAdam, C. Shearer, C. W. Hamilton, et al. (2013). Chromatic mineral identification & surface texture (CMIST) instrument: A next generation contact XRD/XRF tool. 44th Lunar and Planetary Science Conference, Abstract #2116.
- Asal, F., Smith, M., & Priestnall, G. (2000). Combining LIDAR and photogrammetry for urban and rural landscape studies. *The International Archives of the Photogrammetry, Remote Sensing and Spatial Information Sciences*, 33(B3), 44–50.
- Beckhoff, B., Kanngießer, B., Langhoff, N., Wedell, R., & Wolff, H. (Eds) (2006). *Handbook of practical x-ray fluorescence analysis*. New York: Springer. <https://doi.org/10.1007/978-3-540-36722-2>
- Bell, J. F. III, Squyres, S. W., Herkenhoff, K. E., Maki, J. N., Arneson, H. M., Brown, D., et al. (2003). The Mars Exploration Rover Athena Panoramic Camera (Pancam) Investigation. *Journal of Geophysical Research*, 108(E12), 8063. <https://doi.org/10.1029/2003JE002070>
- Bibring, J. P., Langevin, Y., Gendrin, A., Gondet, B., Poulet, F., Berthe, M., et al., & the OMEGA team (2005). Mars surface diversity as revealed by the OMEGA/Mars Express observations. *Science*, 307(5715), 1576–1581. <https://doi.org/10.1126/science.1108806>
- Blake, D., Vaniman, D., Achilles, C., Anderson, R., Bish, D., Bristow, T., et al. (2012). Characterization and calibration of the CheMin Mineralogical Instrument on Mars Science Laboratory. *Space Science Reviews*, 170(1–4), 341–399. <https://doi.org/10.1007/s11214-012-9905-1>
- Blaney, D. L., Wiens, R. C., Maurice, S., Clegg, S. M., Anderson, R. B., Kah, L. C., et al., & the MSL Science Team (2014). Chemistry and texture of the rocks at Rocknest, Gale Crater: Evidence for sedimentary origin and diagenetic alteration. *Journal of Geophysical Research: Planets*, 119, 2109–2131. <https://doi.org/10.1002/2013JE004590>
- Bleacher, J. E., C. W. Hamilton, S. P. Scheidt, W. B. Garry, A. de Wet, P. Whelley, and et al. (2015). No erosion needed: Development of streamlined islands during lava channel construction. Lunar and Planetary Science Conference 46, Abstract #2182.
- Bleacher, J. E., Hurtado, J. M. Jr., Young, K. E., Rice, J. W. Jr., & Garry, W. B. (2013). The effect of different operations modes on science capabilities during the 2010 Desert RATS test: Insights from the geologist crewmembers. *Acta Astronautica*, 90, 356–366. <https://doi.org/10.1016/j.actaastro.2011.10.018>
- Bonthond, G., Merselis, D. G., Dougan, K. E., Graff, T. G., Todd, W., Fourqrean, J. W., & et al. (2018). Inter-domain microbial diversity within the coral holobiont *Siderastrea siderea* from two depth habitats. *PeerJ*, 6, e4324. <https://doi.org/10.7717/peerj.4324>
- Boucher, T., Dyar, M. D., Mahadevan, S., & Clegg, S. M. (2015). Comparison of linear and non-linear approaches to manifold learning predictions of chemical compositions in geological samples using laser-induced breakdown spectroscopy under Mars conditions. *Journal of Chemometrics*, 29(9), 484–491. <https://doi.org/10.1002/cem.2727>
- Brown, R. H., Baines, K. H., Bellucci, G., Bibring, J. -P., Buratti, B. J., Capaccioni, F., et al. (2004). The Cassini Visual and Infrared Mapping Spectrometer (VIMS) investigation. *Space Science Reviews*, 115(1–4), 111–168. <https://doi.org/10.1007/s11214-004-1453-x>
- Carter, W., Shrestha, R., Tuell, G., Bloomquist, D., & Sartori, M. (2001). Airborne laser swatch mapping shines new light on Earth's topography. *Eos, Transactions, American Geophysical Union*, 82(46), 549–555. <https://doi.org/10.1029/01E000321>
- Cashman, K. V., Soule, S. A., Mackey, B. H., Deligne, N. I., Deardorff, N. D., & Dieterich, H. R. (2013). How lava flows: New insights from applications of lidar technologies to lava flow studies. *Geosphere*, 9(6), 1664–1680. <https://doi.org/10.1130/GES00706.1>
- Chemtob, S. M., Jolliff, B. L., Rossman, G. R., Eiler, J. M., & Arvidson, R. E. (2010). Silica coatings in the Ka'u Desert, Hawaii, a Mars analog terrain: A micromorphological, spectral, chemical, and isotopic study. *Journal of Geophysical Research*, 115, E04001. <https://doi.org/10.1029/2009JE003473>
- Chen, Y., Tang, J., Feng, Z., Hakala, T., Hyyppä, J., Zhou, C., et al. (2017). Possibility of applying SLAM-aided LiDAR in deep space exploration. In H. Urbach, & G. Zhang (Eds.), *3rd International Symposium of Space Optical Instruments and Applications*, Springer Proceedings in Physics (Vol. 192, pp. 239–248). New York, NY: Springer.
- Christensen, P. R., Jakosky, B. M., Kieffer, H. H., Malin, M. C., McSween, H. Y. Jr., Neelson, K., et al. (2004). The Thermal Emission Imaging System (THEMIS) for the Mars 2001 Odyssey Mission. *Space Science Reviews*, 110(1/2), 85–130. <https://doi.org/10.1023/B:SPAC.0000021008.16305.94>

- Clegg, S., Wiens, R., Misra, A., Sharma, S., Lambert, J., Bender, S., et al. (2014). Planetary geochemical investigations by Raman-LIBS spectroscopy. *Spectrochimica Acta*, *68*, 925–936. <https://doi.org/10.1366/13-07386>
- Csatho, B., Schenk, T., Kyle, P., Wilson, T., & Krabill, W. B. (2008). Airborne laser swath mapping of the summit of Erebus volcano, Antarctica: Applications to geological mapping of a volcano. *Journal of Volcanology and Geothermal Research*, *177*(3), 531–548. <https://doi.org/10.1016/j.jvolgeores.2008.08.016>
- Devara, P. C. S., Raj, P. E., Sharma, S., & Pandithurai, G. (1995). Real-time monitoring of atmospheric aerosols using a computer-controlled lidar. *Atmospheric Environment*, *29*(16), 2205–2215. [https://doi.org/10.1016/1352-2310\(94\)00355-0](https://doi.org/10.1016/1352-2310(94)00355-0)
- Dyar, M. D., Carmosino, M. L., Tucker, J. M., Brown, E. A., Clegg, S. M., Wiens, R. C., et al. (2012). Remote laser-induced breakdown spectroscopy analysis of East African Rift sedimentary samples under Mars conditions. *Chemical Geology*, *294–295*, 135–151. <https://doi.org/10.1016/j.chemgeo.2011.11.019>
- Dyar, M. D., Tucker, J. M., Humphries, S., Clegg, S. M., Wiens, R. C., & Lane, M. D. (2011). Strategies for Mars remote Laser-Induced Breakdown Spectroscopy analysis of sulfur in geological samples. *Spectrochimica Acta Part B: Atomic Spectroscopy*, *66*(1), 39–56. <https://doi.org/10.1016/j.sab.2010.11.016>
- Eppler, D., Adams, B., Archer, D., Baiden, G., Brown, A., Carey, W., et al. (2013). Desert Research and Technology Studies (DRATS) 2010 science operations: Operational approaches and lessons learned for managing science during human planetary surface missions. *Acta Astronautica*, *90*(2), 224–241. <https://doi.org/10.1016/j.actaastro.2012.03.009>
- Evans, C. A., Calaway, M. J., Bell, M. S., & Young, K. E. (2013). GeoLab—A habitat-based laboratory for preliminary examination of geological samples. *Acta Astronautica*, *90*(2), 289–300. <https://doi.org/10.1016/j.actaastro.2011.12.008>
- Favalli, M., Fornaciai, A., Mazzarini, F., Harris, A., Neri, M., Behncke, B., et al. (2010). Evolution of an active lava flow field using a multitemporal LIDAR acquisition. *Journal of Geophysical Research*, *115*, B11203. <https://doi.org/10.1029/2010JB007463>
- Feigh, K. M., Pritchett, A. R., Denq, T. W., & Jacko, J. A. (2007). Contextual control modes during an airline rescheduling task. *Journal of Cognitive Engineering and Decision Making*, *1*(2), 169–185. <https://doi.org/10.1518/155534307X232839>
- Frodeman, R. (1995). Geological reasoning: Geology as an interpretative and historical science. *Geological Society of America*, *107*(8), 960–968. [https://doi.org/10.1130/0016-7606\(1995\)107<0906:GRGAAI>2.3.CO;2](https://doi.org/10.1130/0016-7606(1995)107<0906:GRGAAI>2.3.CO;2)
- Gellert, R., J. L. Campbell, P. L. King, L. A. Leshin, G. W. Lugmair, J. G. Spray, et al. (2009). The Alpha-Particle-X-ray-Spectrometer (APXS) for the Mars Science Laboratory (MSL) Rover Mission. 40th Lunar and Planetary Science Conference, Abstract #2364.
- Graff, T., K. Young, D. Coan, D. Merselis, A. Bellantuono, K. Dougan, et al. (2017). NEEMO 21: Tools, techniques, technologies & training for science exploration. Lunar and Planetary Science Conference XLVIII, Abstract #2391.
- Graff, T. G., R. V. Morris, S. M. Clegg, R. C. Wiens and R. B. Anderson (2011). Dust removal on Mars using laser-induced breakdown spectroscopy. 42nd Lunar and Planetary Science Conference, Abstract #1916.
- Greeley, R., P. R. Christensen, J. Cantrell, B. C. Clark, R. S. Price, R. M. Zubrin, and et al. (1996). The Mars aerial platform (MAP) concept. 34th Aerospace Sciences Meeting and Exhibit, American Institute of Aeronautics and Astronautics.
- Green, R. O., Pieters, C., Mouroulis, P., Eastwood, M., Boardman, J., Glavich, T., et al. (2011). The moon mineralogy mapper (M3) imaging spectrometer for lunar science: Instrument description, calibration, on-orbit measurements, science data calibration and on-orbit validation. *Journal of Geophysical Research*, *116*, E00G19. <https://doi.org/10.1029/2011JE003797>
- Greenberger, R. N., Mustard, J. F., Ehlmann, B. L., Blaney, D. L., Cloutis, E. A., Wilson, J. H., et al. (2015). Imaging spectroscopy of geological samples and outcrops: Novel insights from microns to meters. *GSA Today*, *25*(12), 4–10. <https://doi.org/10.1130/GSATG252A.1>
- Grotzinger, J. P., Crisp, J., Vasavada, A. R., Anderson, R. C., Baker, C. J., Barry, R., et al. (2012). Mars Science Laboratory Mission and Science Investigation. *Space Science Reviews*, *170*(1–4), 5–56. <https://doi.org/10.1007/s11214-012-9892-2>
- Hamilton, C. W., S. P. Scheidt, J. E. Bleacher, R. P. Irwin III, and W. B. Garry (2015). “Fill and Spill” lava emplacement associated with the December 1974 flow on Kilauea Volcano, Hawaii, USA. Lunar and Planetary Science Conference 46, Abstract #1071.
- Hodges, K. V., & Schmitt, H. H. (2011). A new paradigm for advanced planetary field geology developed through analog exercises on Earth. In W. B. Garry, & J. E. Bleacher (Eds.), *Analog for planetary exploration, Geological Society of America Special Paper*, (Vol. 483). Boulder, CO: Geological Society of America.
- Hoffer, J. (1976). Geology of the Potrillo basalt field. *New Mexico Bureau of Mines & Minerals Research Circular*, *149*, 30.
- Hollnagel, E. (1993). *Human reliability analysis: Context and control*. London: Academic.
- Hurtado, J. M. Jr., Young, K. E., Bleacher, J. E., Garry, W. B., & Rice, J. W. Jr. (2013). Field geologic observation and sample collection strategies for planetary surface exploration: Insights from the 2010 Desert RATS geologist crewmembers. *Acta Astronautica*, *90*(2), 344–355. <https://doi.org/10.1016/j.actaastro.2011.10.015>
- Ito, G., Rogers, A. D., Young, K. E., Bleacher, J. E., Edwards, C. S., Hinrichs, J., et al. (2018). Incorporation of portable infrared spectral imaging into planetary geological field work: Analog studies at Kilauea Volcano, Hawaii and Potrillo Volcanic Field, New Mexico. *Earth and Space Science*, *5*. <https://doi.org/10.1029/2018EA000375>
- Jenkins, R. (1999). *X-ray fluorescence spectrometry*, (2nd ed.). New York: Wiley-Interscience. <https://doi.org/10.1002/9781118521014>
- Jenkins, R., Gould, W. R., & Gedcke, D. (1995). *Quantitative x-ray spectrometry*, (2nd ed.). New York: Marcel Dekker, Inc.
- Jones, A., Bleacher, L., Bleacher, J., Glotch, T., Young, K., Selvin, B., & et al. (2017). Connecting the next generation of science journalists with science in action. *GSA Today*, *27*(1), 44–45.
- Julian, B. and J. Zidek (1991). Field guide to geologic excursions in New Mexico and adjacent areas of Texas and Colorado. New Mexico Bureau of Mines & Mineral Resources, Bulletin 137, Prepared for the Geological Society of America Rock Mountain and South-Central Sections Annual Meeting, Albuquerque, New Mexico, 21–24 April 1991.
- Kastens, K. A., Manduca, C. A., Cervato, C., Frodeman, R., Goodwin, C., Liden, L. S., et al. (2009). How geoscientists think and learn. *Eos, Transactions, American Geophysical Union*, *90*, 265–266. <https://doi.org/10.1029/2009EO310001>
- Klein, G. (2007a). Flexexecution as a paradigm for replanning, part 1. *IEEE Intelligent Systems*, *22*(5), 79–83. <https://doi.org/10.1109/MIS.2007.4338498>
- Klein, G. (2007b). Flexexecution, Part 2: Understanding and Supporting Flexible Execution. *IEEE Intelligent Systems*, *22*, 108–112.
- Larsen, C. F. (2014). Comparisons of Simultaneously Acquired Airborne SfM Photogrammetry and Lidar. American Geophysical Union Fall Meeting 2014, Abstract #C21D-02.
- Levine, J., D. L. Blaney, J. E. P. Connerney, R. Greeley, J. W. Head III, J. H. Hoffman, et al. (2003). Science from a Mars airplane—The Aerial Regional-scale Environmental Survey (ARES) of Mars. 2nd American Institute of Aeronautics and Astronautics “Unmanned Unlimited” Conference, Workshop and Exhibition, American Institute of Aeronautics and Astronautics, DOI:<https://doi.org/10.2514/6.2003-6576>.
- Lockwood, J. P., R. I. Tilling, R. T. Holcomb, F. W. Klein, A. T. Okamura, and D. W. Peterson (1999). Magma migration and resupply during the 1974 summit eruptions of Kilauea Volcano, Hawaii. USGS Professional Paper, 1613.
- Maimone, M., Biesiadecki, J., Tunstel, E., Cheng, Y., & Leger, C. (2004). Surface navigation and mobility intelligence on the Mars Exploration Rovers. In *Intelligence for space robotics*, (pp. 45–70). San Antonio, TX: TSI Press.

- Maimone, M., Jonson, A., Cheng, Y., Willson, R., & Matthies, L. (2006). Autonomous navigation results from the Mars Exploration Rover (MER) Mission. In M. H. Ang, & O. Khatib (Eds.), *Experimental robotics IX*, (Vol. 21, pp. 3–13). Berlin, Heidelberg: Springer. [https://doi.org/10.1007/11552246\\_1](https://doi.org/10.1007/11552246_1)
- Marqui, E., Hidalgo, M., Queralt, I., Van Meel, K., & Fontas, C. (2012). Analytical capabilities of laboratory, benchtop and handheld X-ray fluorescence systems for detection of metals in aqueous samples pre-concentrated with solid-phase extraction disks. *Spectrochimica Acta Part B: Atomic Spectroscopy*, *67*, 17–23. <https://doi.org/10.1016/j.sab.2011.12.004>
- Markey, A. M., Clark, C. S., Succop, P. A., & Roda, S. (2008). Determination of the feasibility of using a portable x-ray fluorescence (XRF) analyzer in the field for measurement of lead content of sieved soil. *Journal of Environmental Health*, *70*, 24–29.
- Maurice, S., Clegg, S., Wiens, R. C., Gasnault, O., Rapin, W., Forni, O., et al. (2016). ChemCam activities and discoveries during the nominal mission of Mars Science Laboratory in Gale crater, Mars. *Journal of Analytical Atomic Spectrometry*, *31*, [https://doi.org/10.1039/C5JA00417A\(4\)](https://doi.org/10.1039/C5JA00417A(4)), 863–889.
- Mazzarini, F., Pareschi, M. T., Favalli, M., Isola, I., Tarquini, S., & Boschi, E. (2007). Lava flow identification and aging by means of lidar intensity: Mount Etna case. *Journal of Geophysical Research*, *112*, B02201. <https://doi.org/10.1029/2005JB004166>
- Meslin, P. Y., Anderson, R., Berger, G., Bish, D., Blake, D., Blaney, D., et al. (2013). Soil diversity and hydration as observed by ChemCam at Gale Crater, Mars. *Science*, *341*. <https://doi.org/10.1126/science.1238670>
- Miller, M. J., A. Claybrook, S. J. Greenlund, and K. M. Feigh (2016). Operational assessment of Apollo lunar surface extravehicular Activity Timeline Execution. AIAA Space Forum 2016, DOI:<https://doi.org/10.2514/6.2016-5391>.
- Ming, D. W., Mittlefehldt, D. W., Morris, R. V., Golden, D. C., Gellert, R., Yen, A., et al., & the Athena Science Team (2006). Geochemical and mineralogical indicators for aqueous processes in the Columbia Hills of Gusev crater, Mars. *Journal of Geophysical Research*, *111*, E02S12. <https://doi.org/10.1029/2005JE002560>
- Morris, A. R., Anderson, F. S., Mouginiis-Mark, P. J., Haldemann, A. F. C., Brooks, B. A., & Foster, J. (2008). Roughness of Hawaiian volcanic terrains. *Journal of Geophysical Research*, *113*, E12007. <https://doi.org/10.1029/2008JE003079>
- Morris, R. V., Vaniman, D. T., Blake, D. F., Gellert, R., Chipera, S. J., Rampe, E. B., et al. (2016). Silicic volcanism on Mars evidenced by tridymite in high-SiO<sub>2</sub> sedimentary rock at Gale crater. *Proceedings of the National Academy of Sciences of the United States of America*, *113*(26), 7071–7076. <https://doi.org/10.1073/pnas.1607098113>
- Murchie, S., Arvidson, R., Bedini, P., Beisser, K., Bibring, J.-P., Bishop, J., et al. (2007). Compact Reconnaissance Imaging Spectrometer for Mars (CRISM) on Mars Reconnaissance Orbiter (MRO). *Journal of Geophysical Research*, *112*, E05S03. <https://doi.org/10.1029/2006JE002682>
- Nachon, M., Clegg, S. M., Mangold, N., Schröder, S., Kah, L. C., Dromart, G., et al. (2014). Calcium sulfate veins characterized by ChemCam/Curiosity at Gale crater, Mars. *Journal of Geophysical Research: Planets*, *119*, 1991–2016. <https://doi.org/10.1002/2013JE004588>
- Norrish, K., & Chappell, B. W. (1977). X-ray fluorescence spectrometry. *Physical Methods in Determinative Mineralogy*, 201–272.
- Norrish, K., & Hutton, J. T. (1969). An accurate X-ray spectrographic method for the analysis of a wide range of geological samples. *Geochimica et Cosmochimica Acta*, *33*(4), 431–453. [https://doi.org/10.1016/0016-7037\(69\)90126-4](https://doi.org/10.1016/0016-7037(69)90126-4)
- Novak, K. S., J. G. Kempenaar, M. Redmond, and P. Bhandari (2015). Preliminary surface thermal design of the Mars 2020 Rover. 45th International Conference on Environmental Systems, ICES-2015-134.
- Ollila, A. M., Newsom, H. E., Clark, B., Wiens, R. C., Cousin, A., Blank, J. G., et al., & the MSL Science Team (2013). Trace element geochemistry (Li, Ba, Sr, and Rb) using Curiosity's ChemCam: Early results for Gale Crater from Bradbury landing site to Rocknest. *Journal of Geophysical Research: Planets*, *119*, 255–285. <https://doi.org/10.1002/2013JE004517>
- Paige, D. A., Foote, M. C., Greenhagen, B. T., Schofield, J. T., Calcutt, S., Vasavada, A. R., et al. (2010). The Lunar Reconnaissance Orbiter Diviner Lunar Radiometer Experiment. *Space Science Reviews*, *150*(1–4), 125–160. <https://doi.org/10.1007/s11214-009-9529-2>
- Parrish, W. (1956). X-ray spectrochemical analysis. *Philips Technical Review*, *17*, 269–286.
- Rampe, E. B., Ming, D. W., Blake, D. F., Bristow, T. F., Chipera, S. J., Grotzinger, J. P., et al. (2017). Mineralogy of an ancient lacustrine mudstone succession from the Murray formation, Gale Crater, Mars. *Earth and Planetary Science Letters*, *471*, 172–185. <https://doi.org/10.1016/j.epsl.2017.04.021>
- Ramsey, M. S., & Harris, A. J. L. (2012). Volcanology 2020: How will thermal remote sensing of volcanic surface activity evolve over the next decade. *Journal of Volcanology and Geothermal Research*, *249*, 217–233.
- Rieder, R., Gellert, R., Bruckner, J., Klingelhofer, G., Dreibus, G., Yen, A., & et al. (2003). The new Athena alpha particle X-ray spectrometer for the Mars Exploration Rovers. *Journal of Geophysical Research*, *108*, 8066. <https://doi.org/10.1029/2003JE002150>
- Rieder, R., Wanke, H., Economou, T., & Turkevich, A. (1997). Determination of the chemical composition of Martian soil and rocks: The alpha proton X-ray spectrometer. *Journal of Geophysical Research*, *102*(E2), 4027–4044. <https://doi.org/10.1029/96JE03918>
- Ross, A., Kosmo, J., & Janoiko, B. (2013). Historical synopses of desert RATS 1997-2010 and a preview of desert RATS 2011. *Acta Astronautica*, *90*(2), 182–202. <https://doi.org/10.1016/j.actaastro.2012.02.003>
- Sarrazin, P., D. Blake, P. Dera, R. Downs, J. Taylor (2017). X-ray diffraction for in-situ mineralogical analysis of planetesimals. American Geophysical Union Fall 2017 Meeting, Abstract #P51B-2599.
- Scheidt, S. P., P. L. Whelley, C. W. Hamilton, J. E. Bleacher, and W. B. Garry (2015). The Kilauea 1974 flow: quantitative morphometry of lava flows using low altitude aerial image data using a kite-based platform in the field. 2015 Fall Meeting, American Geophysical Union, San Francisco, CA, Abstract #P24A-08.
- Schiffman, P., Zierenberg, R., Marks, N., Bishop, J. L., & Dyar, M. D. (2006). Acid-fog deposition at Kilauea volcano: A possible mechanism for the formation of siliceous-sulfate rock coatings on Mars. *Geology*, *34*(11), 921–924. <https://doi.org/10.1130/G22620A.1>
- Schröder, S., Meslin, P. Y., Gasnault, O., Maurice, S., Cousin, A., Wiens, R. C., et al. (2015). Hydrogen detection with ChemCam at Gale Crater. *Icarus*, *249*, 43–61. <https://doi.org/10.1016/j.icarus.2014.08.029>
- Scott, W. E., Sherrod, D. R., & Gardner, C. A. (2008). Overview of 2004 to 2005, and continuing, eruption of Mount St. Helens, Washington. In D. R. Sherrod, W. E. Scott, & P. H. Stauffer (Eds.), *A volcano rekindled: The renewed eruption of Mount St. Helens, 2004-2006, US Geological Survey, US Department of the Interior Professional Paper* (pp. 2–33).
- Seelos, K. D., Arvidson, R. E., Jolliff, B. L., Chemtob, S. M., Morris, R. V., Ming, D. W., & et al. (2010). Silica in a Mars analog environment: Ka'u Desert, Kilauea Volcano, Hawaii. *Journal of Geophysical Research*, *115*, E00D15. <https://doi.org/10.1029/2009JE003347>
- Shaukat, A., Blacker, P., Spiteri, C., & Gao, Y. (2016). Towards camera-LIDAR fusion-based terrain modelling for planetary surfaces: Review and analysis. *Sensors*, *16*(11), 1952. <https://doi.org/10.3390/s16111952>
- Shaw, C. H. (1952). Chemical analysis by X-rays. *The Ohio Journal of Science*, *52*, 134–145.
- Shrivastava, P., O'Connell, S., & Whitley, A. (2005). Handheld x-ray fluorescence spectrometry for archaeologists. In *X ray fluorescence spectrometry (XRF) for geoarchaeology*, (pp. 7–44). New York: Springer.
- Soule, S. A., Cashman, K. V., & Kauahikaua, J. P. (2004). Examining flow emplacement through the surface morphology of three rapidly emplaced, solidified lava flows, Kilauea Volcano, Hawai'i. *Bulletin of Volcanology*, *66*(1), 1–14. <https://doi.org/10.1007/s00445-003-0291-0>

- Squyres, S. W., Arvidson, R. E., Bell, J. F. III, Brückner, J., Cabrol, N. A., Calvin, W., et al. (2004). The opportunity Rover's Athena science investigation at Meridiani Planum, Mars. *Science*, *306*(5702), 1698–1703. <https://doi.org/10.1126/science.1106171>
- Squyres, S. W., Arvidson, R. E., Ruff, S., Gellert, R., Morris, R. V., Ming, D. W., et al. (2008). Discovery of silica-rich deposits on Mars by the Spirit Rover. *Science*, *320*(5879), 1063–1067. <https://doi.org/10.1126/science.1155429>
- Stal, C., Tack, F., de Maeyer, P., de Wulf, A., & Goossens, R. (2013). Airborne photogrammetry and lidar for DSM extraction and 3D change detection over an urban area—A comparative study. *International Journal of Remote Sensing*, *34*(4), 1087–1110. <https://doi.org/10.1080/01431161.2012.717183>
- Sutton, A. J., & Elias, T. (2014). One hundred volatile years of volcanic gas studies at the Hawaiian Volcano Observatory. In M. P. Poland, T. J. Takahashi, & C. M. Landowski (Eds.), *Characteristics of Hawaiian volcanoes, US Geological Survey, US Department of the Interior Professional Paper* (Vol. 1801, pp. 295–322).
- Vaniman, D. T., Bish, D. L., Ming, D. W., Bristow, T. F., Morris, R. V., Blake, D. F., et al., & the MSL Science Team (2014). Mineralogy of a mudstone at Yellowknife Bay, Gale Crater, Mars. *Science*, *343*(6169), 1243480. <https://doi.org/10.1126/science.1243480>
- von Hevesy, G. (1932). *Chemical analysis by X-rays and its applications*. New York: McGraw-Hill.
- Whelley, P. L., Garry, W. B., Hamilton, C. W., & Bleacher, J. E. (2017). LiDAR-derived surface roughness signatures of basaltic lava types at the Muliwai a Pele Lava Channel, Mauna Ulu, Hawai'i. *Bulletin of Volcanology*, *79*(11), 75. <https://doi.org/10.1007/s00445-017-1161-5>
- Whelley, P. L., Glaze, L. S., Calder, E. S., & Harding, D. J. (2014). LiDAR-derived surface roughness texture mapping: Application to Mount St. Helens Pumice plain deposit analysis. *IEEE Transactions on Geoscience and Remote Sensing*, *52*(1), 426–438. <https://doi.org/10.1109/TGRS.2013.2241443>
- Whelley, P. L., Scheidt, S. P., Garry, W. B., Richardson, J., Hamilton, C. W., & Bleacher, J. E. (2017). Comparison and fusion of ultra-high-resolution topographic data at Kilauea volcano, Hawaii. IAVCEI 2017 Scientific Assembly, Fostering Integrative Studies of Volcanoes, August 14–18, Portland, Oregon, U.S.A., Abstract #497, 1219.
- Wiens, R. C., Maurice, S., Barraclough, B., Saccoccio, M., Barkley, W. B., Bell, J. F. III, et al. (2012). The ChemCam instruments on the Mars Science Laboratory (MSL) rover: Body unit and combined system performance. *Space Science Reviews*, *170*(1–4), 167–227. <https://doi.org/10.1007/s11214-012-9902-4>
- Williams, D. R. (2005). The Apollo Lunar Roving Vehicle, NASA. Retrieved from [http://nssdc.gsfc.nasa.gov/planetary/lunar/apollo\\_lrv.html](http://nssdc.gsfc.nasa.gov/planetary/lunar/apollo_lrv.html)
- Yant, M. K., Young, E., Rogers, A. D., McAdam, A. C., Bleacher, J. E., Bishop, J. L., & et al. (2018). Visible, near-infrared, and mid-infrared spectral characterization of Hawaiian fumarolic alteration near Kilauea's December 1974 flow: Implications for spectral discrimination of alteration environments on Mars. *American Mineralogist*, *103*, 11–25.
- Young, K., Hurtado, J. M. Jr., Bleacher, J. E., Garry, W. B., Bleisath, S., Buffington, J., & et al. (2013). Tools and technologies needed for conducting planetary field geology while on EVA: Insights from the 2010 Desert RATS geologist crewmembers. *Acta Astronautica*, *90*(2), 332–343. <https://doi.org/10.1016/j.actaastro.2011.10.016>
- Young, K. E., Bleacher, J. E., Evans, C. A., Arzoumanian, Z., Gendreau, K., & Hodges, K. V. (2014). The integration of handheld technologies into planetary surface exploration. Annual Meeting of the Lunar Exploration Analysis Group (2014), Abstract #3043.
- Young, K. E., Bleacher, J. E., Evans, C. A., Rogers, A. D., Ito, G., Arzoumanian, Z., & Gendreau, K. (2015). Examining volcanic terrains using in situ geochemical technologies: Implications for planetary field geology. 46th Lunar and Planetary Science Conference, Abstract #1658.
- Young, K. E., Evans, C., Allen, C., Mosie, A., & Hodges, K. V. (2011). In-situ XRF measurements in Lunar Surface Exploration using Apollo samples as a standard. 42nd Lunar and Planetary Science Conference, Abstract #2121.
- Young, K. E., Evans, C., & Hodges, K. V. (2012). Evaluating handheld X-ray fluorescence (XRF) technology in planetary exploration: Demonstrating instrument stability and understanding analytical constraints and limits for basaltic rocks. 43rd Lunar and Planetary Science Conference, Abstract #2628.
- Young, K. E., Evans, C. A., Hodges, K. V., Bleacher, J. E., & Graff, T. G. (2016). A review of the handheld X-ray fluorescence spectrometer as a tool for field geologic investigations on Earth and in planetary surface exploration. *Applied Geochemistry*, *72*, 77–87. <https://doi.org/10.1016/j.apgeochem.2016.07.003>
- Young, K. E., T. G. Graff, D. Coan, M. Reagan, W. Todd, A. Naid, et al. (2018). Conducting science-driven extravehicular activities during planetary surface exploration—The NEEMO (NASA Extreme Environment Mission Operations) 22 Mission. 49th Lunar and Planetary Science Conference, Abstract #2422.